

# SPATIAL CONFOUNDING IN MULTIVARIATE AREAL DATA ANALYSIS

KYLE LIN WU AND SUDIPTO BANERJEE

**ABSTRACT.** We investigate spatial confounding in the presence of multivariate disease dependence. In the “analysis model perspective” of spatial confounding, adding a spatially dependent random effect can lead to significant variance inflation of the posterior distribution of the fixed effects. The “data generation perspective” views covariates as stochastic and correlated with an unobserved spatial confounder, leading to inferior statistical inference over multiple realizations. While multiple methods have been proposed for adjusting statistical models to mitigate spatial confounding in estimating regression coefficients, results on interactions between spatial confounding and multivariate dependence are very limited. We contribute to this domain by investigating spatial confounding from the analysis and data generation perspectives in a Bayesian coregionalized areal regression model. We derive novel results that distinguish variance inflation due to spatial confounding from inflation based on multicollinearity between predictors and provide insights into the estimation efficiency of a spatial estimator under a spatially confounded data generation model. We demonstrate favorable performance of spatial analysis compared to a non-spatial model in our simulation experiments even in the presence of spatial confounding and a misspecified spatial structure. In this regard, we align with several other authors in the defense of traditional hierarchical spatial models ([Gilbert et al., 2025](#); [Khan and Berrett, 2023](#); [Zimmerman and Ver Hoef, 2022](#)) and extend this defense to multivariate areal models. We analyze county-level data from the US on obesity / diabetes prevalence and diabetes-related cancer mortality, comparing the results with and without spatial random effects.

## 1. INTRODUCTION

When do spatial effects distort statistical inference for fixed effects? [Hodges and Reich \(2010\)](#) introduced this question in the context of a linear mixed-effects model, arguing that adding a spatially dependent random effect can induce increased estimation bias or variance inflation. They call this phenomenon “spatial confounding.” This notion challenges the conventional wisdom that a spatially dependent random effect should be added when residuals in a non-spatial model exhibit spatial autocorrelation. To mitigate spatial confounding, [Hodges and Reich \(2010\)](#) proposed restricting the spatial effect to the orthogonal complement of the column space of the covariates, which preserves the non-spatial estimates, but faces criticism for inferior inference ([Khan and Calder, 2022](#); [Zimmerman and Ver Hoef, 2022](#)).

Subsequent articles on spatial confounding have typically adopted a “data analysis” or a “data generation” perspective (Khan and Berrett, 2023). Following Hodges and Reich (2010), spatial confounding arises in the analysis perspective from empirical associations between observed explanatory variables and the eigenvectors of an estimated precision matrix. The proposed adjustments include restricted spatial regression (Hodges and Reich, 2010; Hughes and Haran, 2013), restricted spatial GEE (Hui and Bondell, 2022), and SPOCK Prates et al. (2019). On the other hand, spatial confounding occurs in the generation perspective when covariates  $X$  are stochastic, spatially dependent, and correlated with an unobserved confounding effect  $Z$  (Paciorek, 2010). The effects on statistical inference are evaluated across the realizations of the observed dataset. Recent methods that address spatial confounding from a data generation perspective include Spatial+ (Dupont et al., 2022), gSEM (Thaden and Kneib, 2018) and a spectral adjustment introduced by Guan et al. (2023).

This manuscript provides new insights into spatial confounding in the context of Bayesian multivariate spatial regression. Recently, Gilbert et al. (2025) proved the consistency of the generalized least squares spatial estimator under a causal inference framework with random sampling locations and a spatial confounding criterion for data generation. We offer an alternative defense of traditional spatial estimation by focusing our attention on statistical inference from both perspectives for finite samples and fixed sampling locations. Furthermore, studies exploring how multivariate dependencies interact with spatial confounding are somewhat limited. Previous work by Urdangarin et al. (2024) analyzes the Spatial+ adjustment method in multivariate settings, while Azevedo et al. (2021) proposes MSPOCK, a multivariate extension that combines the SPOCK framework with a shared component model. We analyze multivariate dependencies in a coregionalized areal model following Jin et al. (2007) and provide theoretical results on the dependence between variables under maximal spatial smoothing. Our results align with several other articles on the defense of traditional hierarchical spatial models (Gilbert et al., 2025; Khan and Berrett, 2023; Zimmerman and Ver Hoef, 2022). We extend the results therein to multivariate areal models.

Subsequently, Section 2 defines the generation and analysis perspectives in a multivariate spatial modeling context. Section 3 compares the effect of adding a spatial random effect on the posterior distribution of fixed effects in the analysis model and provides conditions for the spatial estimator to improve inference under the generation model, given known variance parameters. Section 4 evaluates the analysis models over multiple simulated datasets on a map of Californian counties with a spatial confounder. Section 5 compares non-spatial and spatial analysis of data on obesity and diabetes prevalence at the county level in the US alongside diabetes-related cancer mortality rates. Section 6 concludes with a discussion.

## 2. DATA GENERATION AND ANALYSIS MODELS

**2.1. Data Generation Model with Spatial Confounder.** Let  $Y_i$  be an  $n \times 1$  vector corresponding to the  $i$ th outcome for each  $i = 1, \dots, k$ ,  $X_1 = [X_{11}, \dots, X_{1p}]$ , be an  $n \times p$  matrix of predictors, and

$Z_i$  be an  $n \times 1$  vector of unknown confounding effects. We assume data is generated from a model associating  $Y_i$ ,  $X_1$  and  $Z_i$  as

$$Y_i = \beta_{0i}1_n + X_1\beta_{1i} + Z_i + \eta a_i, \quad Z_i = \delta_{0i}1_n + X_1\delta_{1i} + \zeta a_i, \quad X_{1j} = \mu_j 1_n + \epsilon c_j, \quad (1)$$

for each  $i = 1, \dots, k$  and  $j = 1, \dots, p$ . The three equations in (1) represent models for  $[Y | X_1, Z]$ ,  $[Z | X_1]$ , and  $[X_1]$ . Scalar intercepts for  $Y_i$ ,  $Z_i$ , and  $X_{1j}$  are denoted by  $\beta_{0i}$ ,  $\delta_{0i}$ , and  $\mu_j$ , respectively;  $1_n$  is the  $n \times 1$  vector of ones; and  $\beta_{1i}$  and  $\delta_{1i}$  are  $p \times 1$  vectors of fixed regression coefficients. The distributions in the first two models are specified using  $n \times k$  matrices  $\eta = [\eta_1, \dots, \eta_k]$  and  $\zeta = [\zeta_1, \dots, \zeta_k]$  with random zero mean error terms and a shared fixed vector  $k \times 1$   $a_i$ . The distribution in the third model is specified by  $\epsilon = [\epsilon_1, \dots, \epsilon_p]$ , which is  $n \times p$  with random zero-mean error terms, and constant coefficients comprising the  $p \times 1$  vector  $c_j$ . The predictors in  $X_1$  influence each response  $Y_i$  directly through  $\beta_{1i}$  and through the unobserved confounding effects  $Z_i$ .

Letting  $Y = [Y_1, \dots, Y_k]$  and  $Z = [Z_1, \dots, Z_k]$  be  $n \times k$  matrices, we rewrite (1) as

$$Y = 1_n\beta_0^T + X_1\beta_1 + Z + \eta A, \quad Z = 1_n\delta_0^T + X_1\delta_1 + \zeta A, \quad X_1 = 1_n\mu^T + \epsilon C, \quad (2)$$

where  $\beta_1$  and  $\delta_1$  are  $p \times k$  with  $i$ th columns  $\beta_{1i}$  and  $\delta_{1i}$ , respectively;  $\beta_0 = (\beta_{01}, \dots, \beta_{0k})^T$  and  $\delta_0 = (\delta_{01}, \dots, \delta_{0k})^T$  are  $k \times 1$ ; and  $A = [a_1, \dots, a_k]$  and  $C = [c_1, \dots, c_p]$  are  $k \times k$  and  $p \times p$ , respectively, and assumed to be invertible. We assume that  $\eta$ ,  $\zeta$ , and  $\epsilon$  are statistically independent and the columns of  $\eta$  and  $\zeta$  are independent. Hence,  $A$  induces the dependence between outcomes in the columns of  $Y$  and  $Z$ , while  $C$  specifies the dependence between columns of  $X_1$ . Spatial associations between the columns of  $Y$ ,  $Z$ , and  $X_1$  arise from the dependence between the columns of  $\eta$ ,  $\zeta$ , and  $\epsilon$ , respectively, or any combination of them.

The vector  $\text{vec}(Y)$  is  $nk \times 1$  obtained by stacking columns of  $Y$  and has variance  $\text{Var}(\text{vec}(Y)) = (A^T \otimes I_n) \text{Var}(\text{vec}(\eta + \zeta))(A \otimes I_n) + (C^T \otimes I_n) \text{Var}(\text{vec}(\epsilon))(C \otimes I_n)$ , where  $\otimes$  denotes the Kronecker product and  $I_n$  is the identity matrix  $n \times n$ . Since the columns of  $\eta$ ,  $\zeta$ , and  $\epsilon$  are independent,  $\text{Var}(\text{vec}(\eta + \zeta))$  is  $nk \times nk$  block diagonal with  $k$  diagonal block elements, and  $\text{Var}(\text{vec}(\epsilon))$  is  $np \times np$  block diagonal with  $p \times p$  diagonal blocks. We focus on spatially dependent  $X_1$  and  $Z$  by introducing spatial structure in the diagonal blocks of  $\text{Var}(\text{vec}(\zeta))$  and  $\text{Var}(\text{vec}(\epsilon))$ .

For a univariate outcome, the BYM (Besag, York and Mollié) model and the BYM2 reparameterization introduced in [Riebler et al. \(2016\)](#) are flexible classes of spatial analysis models that incorporate spatial and non-spatial error variances. Multivariate areal data analysis for dependent outcomes has a substantial following in epidemiology (see [Gao et al., 2022](#); [MacNab, 2016, 2018](#), and references therein for different approaches). Following [Jin et al. \(2007\)](#), we extend the BYM2 model to the multivariate setting by modeling the error terms of  $X_1$  and  $Z$  as linear transformations of independent latent univariate BYM2 spatial processes. Let  $V_\phi$  be a fixed positive definite  $n \times n$  matrix that encodes spatial autocorrelation,  $P$  be a diagonal  $k \times k$  matrix with diagonal elements  $\rho_i \in (0, 1)$ , and  $0_n$  be an  $n \times 1$  vector of zeroes. The columns of the latent error terms  $\{\eta, \zeta, \epsilon\}$  are modeled as

$$\eta_i \sim N_n(0_n, (1 - \rho_i)I_n), \quad \zeta_i \sim N_n(0_n, \rho_i V_\phi), \quad \epsilon_j \sim N_n(0_n, V_\phi), \quad (3)$$

for  $i = 1, \dots, k$  and  $j = 1, \dots, p$ . Then (2) implies  $\text{Var}(\text{vec}(Y) | X_1) = A^T(I_k - P)A \otimes I_n + A^T P A \otimes V_\phi$ . Conditional on  $X_1$ , variation in  $Y$  stems from  $(\epsilon + \zeta)A$ , and  $\text{Var}(\epsilon_i + \zeta_i) = (1 - \rho_i)I_n + \rho_i V_\phi$ . Thus,  $\rho_i$  can be interpreted as the spatial proportion of the error variance in the  $i$ th latent spatial process conditional on  $X_1$  when  $V_\phi$  is scaled so that the geometric mean of the marginal variances is approximately one, similar to the univariate BYM2 model (Riebler et al., 2016);  $A$  functions both as a scaling and linear transformation from the latent error terms to the observed data. Since  $\text{Cov}(Z_i, \text{vec}(X_1)) = \delta_{1i}^T C^T C \otimes V_\phi$ , we define  $Z_i$  as a spatial confounder if  $\delta_{1i} \neq 0_p$ .

**2.2. Spatial and Non-Spatial Bayesian Analysis Models.** We estimate  $\beta = (\beta_0, \beta_1^T)^T$  using non-spatial and spatial analysis models. For the former, we employ a conjugate Bayesian multivariate regression analysis model,

$$Y = X\beta_{NS} + v_{NS}, \quad \text{vec}(v_{NS}) \sim N_{nk}(0_{nk}, \Sigma_{NS} \otimes I_n), \quad \pi(\beta_{NS}, \Sigma_{NS}) \propto \text{IW}(\Sigma_{NS} | v, v\Sigma_0), \quad (4)$$

where the design matrix  $X = (1_n, X_1)$  is full column rank,  $\beta_{NS}$  is the  $(p + 1) \times k$  vector of slopes,  $\Sigma_{NS}$  is  $k \times k$  and encodes between-outcome covariance, and the prior  $\pi(\beta_{NS}, \Sigma_{NS})$  is uninformative on  $\beta$  while placing an inverse-Wishart distribution on  $\Sigma_0$  with degrees of freedom  $v > k - 1$  and  $k \times k$  scale matrix  $\Sigma_0$  specifying the mean  $\mathbb{E}[\Sigma_{NS}^{-1}] = \Sigma_0^{-1}$ . We denote parameters in the analysis model with a subscript to emphasize a separation from the fixed unknown parameters in the data generating model in (2). The joint posterior is

$$\pi(\beta_{NS}, \Sigma_{NS} | Y, X_1) = \underbrace{\text{IW}(v_\star, \Sigma_\star)}_{p(\Sigma_{NS} | Y, X_1)} \times \underbrace{N_{pk}\left(\text{vec}\left(\widehat{\beta}_{NS}\right), \Sigma_{NS} \otimes (X^T X)^{-1}\right)}_{p(\beta_{NS} | \Sigma_{NS}, Y, X_1)}, \quad (5)$$

where  $\widehat{\beta}_{NS} = (X^T X)^{-1} X^T Y$ ,  $v_\star = v + n$  and  $\Sigma_\star = v\Sigma_0 + (Y - X\widehat{\beta}_{NS})^T (Y - X\widehat{\beta}_{NS})$ . Exact samples from  $\pi(\beta_{NS}, \Sigma_{NS} | Y, X_1)$  are obtained by simulating  $\Sigma_{NS} \sim \text{IW}(v_\star, \Sigma_\star)$  and then drawing a value of  $\beta_{NS} \sim N_{pk}\left(\text{vec}\left(\widehat{\beta}_{NS}\right), \Sigma_{NS} \otimes (X^T X)^{-1}\right)$  for each drawn value of  $\Sigma_{NS}$ .

Turning to spatial analysis, we consider a multivariate BYM2 parameterization of a spatial random effect by writing the spatial analysis model as

$$Y = X\beta_S + \gamma + v_S, \quad \gamma = \Phi M, \quad v_S = \Psi M, \quad \Phi = (\phi_1, \dots, \phi_k), \quad \Psi = (\psi_1, \dots, \psi_k), \quad (6)$$

$$\phi_i \stackrel{\text{ind.}}{\sim} N_n(0_n, r_i V_\phi), \quad \psi_i \stackrel{\text{ind.}}{\sim} N_n(0_n, (1 - r_i)I_n) \quad \text{for } i = 1, \dots, k,$$

where  $\gamma$  is  $n \times k$  comprising spatial effects,  $M$  is  $k \times k$  and invertible that induces correlation between outcomes,  $W_\phi$  is known  $n \times n$  and positive definite capturing spatial autocorrelation, and  $R = \text{diag}(r_1, \dots, r_k)$  with  $r_i \in (0, 1)$  for  $i = 1, \dots, k$ . The analysis parameters  $\{\beta_S, M, R\}$  mimic the role of  $\{\beta, A, P\}$  in the data-generation model, while the spatial structure of  $W_\phi$  parallels  $V_\phi$ . Latent spatial structure is introduced by constructing  $W_\phi^{-1}$  using, for example, the conditionally autoregressive model (CAR), simultaneous autoregressive model (SAR), or the directed acyclic graph auto-regressive model (DAGAR) developed in Datta et al. (2019).

We specify the prior for (6) as  $\pi(\beta_S, \gamma, M, R) = N_{nk}(\text{vec}(\gamma) | 0_{nk}, M^T R M \otimes W_\phi) \times \pi(M) \times \pi(R)$ . For  $\pi(M)$  we let  $\Sigma_S = M^T M$ , where  $M$  is the upper-triangular Cholesky factor, and set  $\pi(\Sigma_S) =$

$\text{IW}(\Sigma_S | v, v\Sigma_0)$  such that  $\mathbb{E}[\Sigma_S^{-1}] = \Sigma_0^{-1}$ . Hence,  $\pi(M) \propto \text{IW}(M^T M | v, v\Sigma_0) \times \prod_{i=1}^k M_{ii}^{k-i+1}$ , where  $\prod_{i=1}^k M_{ii}^{k-i+1}$  is proportional to the Jacobian  $\left| \frac{\partial \Sigma_S}{\partial M_{ij}} \right|$ . Following (Simpson et al., 2017), we specify a penalized complexity (PC) prior  $\pi(R) = \text{PC}(R | \lambda_R) \propto \lambda_R \exp(-\lambda_R \sqrt{2\text{KLD}(R)})$  that encourages model parsimony and robustness, where  $\lambda_R > 0$  is a flexibility hyperparameter and  $\text{KLD}(R)$  is the Kullback-Leiber divergence of  $N_{nk}(0, (I_k - R) \otimes I_n + R \otimes W_\phi)$  from  $N_{nk}(0, I_{nk})$ . Here,  $2\text{KLD}(R) = -n \sum_{i=1}^k r_i + \left( \sum_{i=1}^k r_i \right) \left( \sum_{j=1}^n \lambda_j^{-1} \right) - \sum_{i=1}^k \sum_{j=1}^n \log(1 - r_i + r_i \lambda_j^{-1})$ , where  $\lambda_1, \dots, \lambda_n$  are the eigenvalues of  $W_\phi^{-1}$ . This produces

$$\begin{aligned} \pi(\beta_S, \gamma, M, R) &\propto N_{nk}(\text{vec}(\gamma) | 0, M^T R M \otimes W_\phi) \\ &\times \text{IW}(M^T M | v, v\Sigma_0) \times \text{PC}(R | \lambda_R) \times \prod_{i=1}^k M_{ii}^{k-i+1}. \end{aligned} \quad (7)$$

For tractable analysis, we consider the posterior mean of  $\beta_S$  conditioned on  $M$  and  $R$  as a point estimator for  $\beta$ . Section 3.1 characterizes spatial confounding in the spatial analysis model through the posterior variance of  $\beta_S$  and bias of the conditioned spatial estimator for fixed  $(X_1, Z)$ , similar to the original analysis of Hodges and Reich (2010). Section 3.2 shows that in the presence of a spatial confounder  $Z$ , the conditioned spatial estimator nevertheless retains superior estimation performance compared to the non-spatial estimator under the data generation model in (2).

### 3. MULTIVARIATE SPATIAL CONFOUNDING

**3.1. Spatial Confounding in the Analysis Model.** Under the non-spatial analysis model in (4), a natural point estimate for  $\beta$  is  $\widehat{\beta}_{NS} = \mathbb{E}[\beta_{NS} | Y, X_1] = (X^T X)^{-1} X^T Y$ , which is equivalent to separate univariate ordinary least squares estimates for each outcome. Since  $\widehat{\beta}_{NS}$  does not depend on  $\Sigma_{NS}$ , the dependence between the outcomes does not have an effect on the point estimate of  $\beta$  and, subsequently, the bias introduced by the confounder  $Z$ . Under the data generation model in (2),

$$\text{Bias}(\widehat{\beta}_{NS} | X_1, Z) = \mathbb{E}[\widehat{\beta}_{NS} - \beta | X_1, Z] = (X^T X)^{-1} X^T Z. \quad (8)$$

For the spatial analysis model given by (6), let  $H = X(X^T X)^{-1} X^T$ ,  $B_1 = I_k \otimes (X^T X)^{-1} X^T$ ,  $B_2^{-1} = M^{-1}(I_k - R)^{-1} M^{-T} \otimes (I - H) + M^{-1} R^{-1} M^{-T} \otimes W_\phi^{-1}$ , and  $\widehat{\gamma} = \mathbb{E}[\gamma | Y, M, R, X_1]$ . Derivation of the conditional posterior  $\pi(\beta_S, \gamma | Y, M, R, X_1)$  in Appendix A reveals that  $\text{vec}(\beta_S) | Y, M, R, X_1 \sim N_{pk}(\text{vec}(\widetilde{\beta}_S), M^T(I_k - R)M \otimes (X^T X)^{-1} + B_1 B_2 B_1^T)$  where the conditional spatial estimator  $\widetilde{\beta}_S = \mathbb{E}[\beta_S | Y, M, R, X_1]$  is

$$\widetilde{\beta}_S = \widehat{\beta}_{NS} - (X^T X)^{-1} X^T \widehat{\gamma}, \quad \text{vec}(\widehat{\gamma}) = (M^T \otimes I_n) B^{-1} \text{vec} \left( (I_n - H) Y M^{-1} \right), \quad (9)$$

and  $B = I_k \otimes (I_n - H) + R^{-1}(I_k - R) \otimes W_\phi^{-1}$ . The term  $(X^T X)^{-1} X^T \widehat{\gamma}$  illuminates the exact contribution of adding a spatial effect to the estimation of  $\beta$  that is derived from an inseparable interaction of latent spatial autocorrelation and dependence between results through  $W_\phi^{-1}$ ,  $M$ , and  $R$ . The spatial effects  $\gamma$  absorb spatial information from  $Y$  through the residuals  $(I_n - H)Y$ , as  $\widetilde{\beta}_S$  can be interpreted as the estimate of  $\beta$  under the non-spatial model in (4) with  $Y_\star = Y - \mathbb{E}[\gamma | Y, M, R, X_1]$  as the

response instead of  $Y$ . Similar to how restricted spatial regression preserves the non-spatial estimate of  $\beta$  under a spatial model, the non-spatial estimator can be recovered under the spatial analysis model in (6) by the relation  $\widehat{\beta}_{NS} = \mathbb{E}[\beta_S + (X^T X)^{-1} X^T \gamma \mid Y, M, R, X_1]$ .

An immediate consequence of (9) is that the bias of  $\widetilde{\beta}_S$  under (2) can be decomposed as

$$\begin{aligned} \text{vec}(\text{Bias}(\widetilde{\beta}_S \mid X_1, Z)) &= \text{vec}(\text{Bias}(\widehat{\beta}_{NS} \mid X_1, Z)) \\ &\quad - (M^T \otimes (X^T X)^{-1} X^T) B^{-1} \text{vec}((I_n - H) Z M^{-1}), \end{aligned} \quad (10)$$

where the second term is the additional bias induced by the addition of the spatial effects  $\gamma$ . If the columns of  $Z$  are linear combinations of the columns of  $X$ , then  $(I - H)Z = 0$  and  $\text{Bias}(\widetilde{\beta}_S) = \text{Bias}(\widehat{\beta}_{NS})$ . Bias already exists in the non-spatial model from collinearity between  $X$  and  $Z$ , and the spatial random effect adjusts the bias based on a product between  $X$  and the projection of  $Z$  onto the orthogonal complement of  $X$  that is weighted according to both spatial structure and between-outcome covariance. Whether or not the adjustment exacerbates or counterbalances the non-spatial bias depends on the exact structure of  $X$  and  $Z$ . The non-spatial estimator  $\widehat{\beta}_{NS}$  is unbiased if and only if  $X^T Z = 0$ , while  $\widetilde{\beta}_S$  is unbiased if and only if  $\text{vec}(X^T Z) = (M^T \otimes X^T) B^{-1} \text{vec}((I - H) Z M^{-1})$ .

Hodges and Reich (2010) argue that severe variance inflation from spatial confounding occurs when the ratio of non-spatial to spatial variance is near 0. We show that the inflation of  $\text{Var}(\text{vec}(\beta_S) \mid Y, M, R, X_1)$  in the analysis model given by (6) is limited when  $W_\phi^{-1}$  is positive definite. By spectral decomposition, there exist an orthogonal matrix  $Q \in \mathbb{R}^{n \times n}$  and a diagonal matrix  $D = \text{diag}(d_1, \dots, d_n)$  with  $d_i \geq 0$  for all  $i = 1, \dots, n$  such that  $W_\phi^{1/2} (I - H) W_\phi^{1/2} = Q D Q^T$ . The derivations in Appendix A reveal that  $\text{Var}(\text{vec}(\beta_S) \mid Y, M, R, X_1) = M^T (I_k - R) M \otimes (X^T X)^{-1} + S ((I_k - R)^{-1} \otimes D + R^{-1} \otimes I_n)^{-1} S^T$ , where  $U = W_\phi^{1/2} Q$  and  $S = M^T \otimes (X^T X)^{-1} X^T U$ . Let  $R = r I_k$  such that  $r \in (0, 1)$  represents the proportion of spatial variation. Spatial smoothing increases as  $r \rightarrow 1^-$ , but for any  $d_i$ ,  $\lim_{r \rightarrow 1^-} \frac{1}{1/r + d_i/(1-r)} = I(d_i = 0)$ , where  $I(\cdot)$  is the indicator function. Let  $D^*$  be a  $n \times n$  diagonal matrix such that  $D_{ii}^* = I(d_i > 0)$  for  $i = 1, \dots, n$ . Then,  $\lim_{r \rightarrow 1^-} ((I_k - R)^{-1} \otimes D + R^{-1} \otimes I_n)^{-1} = I_k \otimes (I_n - D^*)$  and the posterior conditional variance approaches the limit

$$\lim_{r \rightarrow 1^-} \text{Var}(\text{vec}(\beta_S) \mid Y, M, r, X_1) = M^T M \otimes (X^T X)^{-1} X^T (W_\phi - U D^* U^T) X (X^T X)^{-1}, \quad (11)$$

suggesting that setting  $W_\phi^{-1}$  as positive definite guards against extreme variance inflation from spatial confounding. Furthermore,  $\lim_{r \rightarrow 1^-} \widetilde{\beta}_S = \widehat{\beta}_{NS} - (X^T X)^{-1} X^T U D^* U^{-1} Y$  from similar calculations. In a univariate BYM2 model, Wu and Banerjee (2025) provides the limiting distribution of the total error variance as the smoothing ratio approaches zero. In our setting, the limiting distribution of  $M^T M$ , derived in Appendix B as

$$\lim_{r \rightarrow 1^-} \pi(M^T M \mid Y, r, X_1) = \text{IW}(M^T M \mid \nu + n - p - 1, \nu \Sigma_0 + Y^T U^{-T} D^* U^{-1} Y), \quad (12)$$

illuminates the limiting effect of maximal spatial smoothing on the scale of the conditional variance and between-outcome dependence. The asymptotic results of (11) and (12) indicate that the posterior variance of  $\beta_S$  does not explode when the noise-to-signal ratio is near zero, contradicting the argument of [Hodges and Reich \(2010\)](#) that variance inflation from spatial confounding is comparable to multicollinearity in linear models. Statistical inference remains intact under extreme spatial smoothing, unlike the pathological case of perfect multicollinearity in covariates. Analysts should assess the degree of spatial smoothing present in the data to assess whether the spatial effect is problematic for the spatial analysis model.

Multiple authors point out that restricted spatial regression can lead to misleading statistical inference. For example, [Khan and Calder \(2022\)](#) shows that the marginal posterior variance in restricted spatial regression is less than the posterior variance in a non-spatial model, contradicting a central hypothesis of restricted spatial regression models. From a frequentist data-generation perspective, [Zimmerman and Ver Hoef \(2022\)](#) points out that conditional on the variance parameter, restricted spatial regression underestimates the variability of the fixed effects' estimator in the true data generation model. In the following section, we reinforce the notion that restricted spatial regression methods are unnecessary by showing that under the data generation model given by (2), the Bayesian spatial estimator  $\tilde{\beta}_S$  is more efficient than the non-spatial estimator  $\hat{\beta}_{NS}$ . We connect the analysis model and the data generation perspectives by demonstrating that the posterior variance in the analysis model captures the estimator's variance in the data generation model.

**3.2. Statistical Inference Over Multiple Datasets.** Although predictors are often considered as fixed variables when evaluating estimation of the fixed effects  $\beta$ , treating  $X_1$  as stochastic is also logical when covariates, such as population characteristics, are measured or estimated with finite precision. Hence, we consider the bias and mean-squared error of point estimates of  $\beta$  over repeated realizations of  $(X_1, Z, Y)$  to account for the variance in the predictors and confounding effects. If the data generation model satisfies  $\mathbb{E}[Z | X_1] = X\delta$ , where  $\delta$  is any  $(p+1) \times k$  matrix, then (10) implies  $\mathbb{E}[\tilde{\beta}_S] = \mathbb{E}[\hat{\beta}_{NS}] = \beta + \delta$ , where the expectation is taken over the joint distribution of  $(X_1, Y, Z)$ . In this case,  $\tilde{\beta}_S$  and  $\hat{\beta}_{NS}$  are equally biased regardless of the values of  $M$ ,  $R$ , and  $W_\phi^{-1}$  used to construct  $\tilde{\beta}_S$ . Analysis in Appendix C reveals that if  $\text{Var}(\text{vec}(Y) | X_1) = A^T P A \otimes V_\phi + A^T (I_k - P) A \otimes I_n$ ,  $V_\phi = W_\phi$ , and  $\tilde{\beta}_S = \mathbb{E}[\beta_S | Y, M = A, R = P, X_1]$ , then  $\text{Var}(\tilde{\beta}_{S,ij} | X_1) < \text{Var}(\hat{\beta}_{NS,ij} | X_1)$ , and if  $\mathbb{E}[Z | X_1] = X\delta$  as well,

$$\text{Var}(\tilde{\beta}_{S,ij}) < \text{Var}(\hat{\beta}_{NS,ij}) \text{ and } \mathbb{E} \left[ (\tilde{\beta}_{S,ij} - \beta_{ij})^2 \right] < \mathbb{E} \left[ (\hat{\beta}_{NS,ij} - \beta_{ij})^2 \right] \quad (13)$$

for all  $i = 0, \dots, p$  and  $j = 1, \dots, k$ . In other words, if the variance structure of the spatial analysis model matches the data generation model and the conditional mean of  $Z$  is a linear transformation of  $X$ , then  $\tilde{\beta}_S$  is always a more efficient estimator than  $\hat{\beta}_{NS}$  in terms of mean squared error over repeated realizations of  $(X_1, Y, Z)$ . In multivariate analysis, this result depends both on the correct specification of the latent spatial variance structure and the correlation between outcomes. [Paciorek \(2010\)](#) argues that a classical spatial model does not adjust for confounding because it does not

reduce bias compared to ordinary least squares. In our setting, this is true when the conditional mean of  $Z$  is a linear transformation of  $X$ , a common assumption in research on spatial confounding from the data generation perspective (Dupont et al., 2022; Thaden and Kneib, 2018), but the benefit of the spatial analysis model is a potential reduction in the estimator’s variance, not bias.

The conditions for (13) hold for the data generation model discussed in (2) and (3) with  $\delta = (\delta_0, \delta_1^T)^T$ . So, the estimator  $\tilde{\beta}_S = \mathbb{E}[\beta_S | Y, M = A, R = P, X_1]$  from the spatial analysis model is preferable to  $\hat{\beta}_{NS}$ . If  $V_\phi^{-1} = W_\phi^{-1}$ , the variance of  $\tilde{\beta}_S$  in the data generation model is equal to the posterior variance in the analysis model given the true data generation parameters,

$$\text{Var}(\text{vec}(\tilde{\beta}_S) | X_1) = \text{Var}(\text{vec}(\beta_S) | Y, M = A, R = P, X_1), \quad (14)$$

where the left term is evaluated under the data generation model in (2) and the right term is evaluated under the spatial analysis model in (6) (see Appendix C for a proof). If  $\tilde{\beta}_S$  is unbiased (i.e.  $\delta = 0_{(p+1) \times k}$ ), credible intervals constructed using the conditional posterior will have coverage probability equal to the nominal coverage rate across realizations of  $(Z, Y)$  with  $X_1$  fixed. However,  $\tilde{\beta}_S$  cannot be calculated if  $A$  and  $P$  are not known. For fully Bayesian inference, one solution is to use the marginal posterior mean of  $\beta$  under (6), which we denote as  $\hat{\beta}_S = \mathbb{E}[\beta_S | Y]$ . A natural question is whether  $\hat{\beta}_S$  improves the estimation of  $\beta$  under assumptions on the data-generating model similar to the case of  $\tilde{\beta}_S$ . Because  $\hat{\beta}_S$  does not have a closed-form expression, we conduct simulation experiments to assess estimation performance and robustness of the analysis model under misspecified spatial structure.

#### 4. SIMULATION ANALYSIS OF SPATIAL ESTIMATOR

We generate data sets  $D^{(i)} = \{X_1^{(i)}, Y^{(i)}\}$  using (2), where  $X_1^{(i)}$  is a  $58 \times 1$  vector and  $Y^{(i)}$  is a  $58 \times 3$  matrix of  $k = 3$  outcomes generated on a map of the  $n = 58$  California counties for  $i = 1, \dots, 300$ . We set  $\beta_0 = (0, 2, 4)^T$  and  $\beta_1 = (1, 3, 5)^T$ ,  $\delta_0 = (0.4375, 0.375, 0.4375)^T$ ,

$$\delta_1^T = (0.125, 0.25, 0.125)^T, \mu = 0.5, \mu_Z = 0.5, A = \begin{bmatrix} -0.5 & -0.5 & 1.5 \\ 1.25 & -1.25 & 0 \\ 1.5 & 1.5 & 1.5 \end{bmatrix} \text{ such that } \Sigma = A^T A =$$

$$\begin{bmatrix} 4.0625 & 0.9375 & 1.5 \\ 0.9375 & 4.0625 & 1.5 \\ 1.5 & 1.5 & 4.5 \end{bmatrix}, P = \text{diag}(0.9, 0.7, 0.4), \text{ and } C = 2. \text{ To induce spatial dependence, we}$$

specify a conditionally autoregressive (CAR) structure,  $V_\phi^{-1} = c(D_W - \alpha W)$ , where  $W$  is the adjacency matrix,  $D_W$  is a diagonal matrix with each diagonal element  $D_{W,ii}$  being the number of neighbors of county  $i$ ,  $\alpha$  is the spatial smoothing parameter, and  $c$  is a scaling factor such that the geometric mean of the diagonal elements of  $W_\phi^{-1}$  is equal to one. We set  $\alpha = 0.99$  and  $c = 0.8352$  to construct  $V_\phi^{-1}$  using the map of the 58 Californian counties.

For the spatial analysis model in (6), we employ the CAR prior through (7) with  $W_\phi = V_\phi$ , and refer to this model as the unconditioned CAR model. Following the suggestion of Jin et al.

(2007), we set  $\nu = 3$  for all simulation runs and  $\Sigma_0$  as a diagonal matrix with diagonal entries equal to  $\|(I_n - H)Y_j\|^2 / (n - p - 1)$ . Although the prior  $\pi(\Sigma_S)$  is dependent on the data, Jin et al. (2007) argues that this enables robust posterior inference. We fix  $\lambda_R = 0.01$  for  $\pi(R)$ , a vague prior on  $R$  that attributes slightly higher prior density to smaller values of  $r_i$ . The spatial estimates  $\widehat{\beta}_S^{(i)}$  and 95% highest posterior density credible intervals for each fixed effect are computed using 20,000 posterior samples of  $\beta_S$  after 20,000 burn-in samples obtained through a Metropolis within Gibbs sampling scheme detailed in Appendix D with proposal settings  $s_1 = 0.10$ ,  $s_2 = 0.15$ , and  $s_3 = 0.25$ . For the conditioned CAR model, we calculate  $\widetilde{\beta}^{(i)}$  using (9) by setting  $M$ ,  $R$ , and  $W_\phi$  equal to the true simulation values of  $A$ ,  $P$ , and  $V_\phi$ , respectively. We compute 95% conditional credible intervals as  $\widetilde{\beta}_{ij} \pm z_{0.975} \sqrt{\text{Var}(\beta_{S,ij} | Y, X_1, A, P)}$  for  $i = 0, \dots, p$  and  $j = 1, \dots, k$ . For the non-spatial model in (4), we set  $\pi(\beta_{NS}, \Sigma_{NS}) \propto \text{IW}(\Sigma_{NS} | \nu, \nu\Sigma_0)$  with the hyperparameters  $\nu = 3$  and  $\nu\Sigma_0$  identical to the scale matrix for  $\pi(\Sigma_S)$ . We calculate 95% highest posterior density credible intervals for each fixed effect using 10,000 exact posterior samples from  $\pi(\beta_{NS}, \Sigma_{NS} | Y, X_1)$ . To examine the effects of misspecifying the spatial prior, we evaluate the aforementioned estimates and credible intervals under a SAR spatial prior on  $\gamma$  by setting  $W_\phi^{-1} = c(I_n - \alpha\widetilde{W})(I_n - \alpha\widetilde{W})^\top$  where  $\widetilde{W}$  is a row-normalization of  $W$  such that  $\widetilde{W}_{ij} = W_{ij} / \sum_{m=1}^n W_{im}$ ,  $\alpha = 0.99$  is the spatial smoothing parameter, and  $c = 220.1809$  is a scaling factor such that the geometric mean of the prior marginal variances is equal to one.

The frequentist evaluation of the posterior means and 95% credible intervals for each analysis model in Table 1 provides simulation evidence for the claim of (13), as the conditional spatial estimator  $\widetilde{\beta}_S$  is superior to  $\widehat{\beta}_{NS}$  in terms of mean squared error for every coefficient despite the presence of the spatial confounder  $Z$  in the data generation model. Although  $\widehat{\beta}_S$  has slightly higher mean squared error than  $\widetilde{\beta}_S$  due to its construction without knowledge of  $A$  and  $P$ ,  $\widetilde{\beta}_S$  has lower mean squared error for every coefficient than the non-spatial estimator  $\widehat{\beta}_{NS}$ . The spatial model has larger frequentist averages of the posterior variance, especially for the intercept terms  $\beta_0$ . However, the spatial model retains frequentist coverage closer to the nominal level of the credible interval while the non-spatial model does not yield a coverage rate above 0.75 for any coefficient. This illustrates that the multivariate spatial analysis model in (6) can improve estimation compared to the non-spatial analysis model in (4) despite the effects of spatial confounding and uncertainty about the variance parameters  $A$  and  $P$ . Increased posterior variance in the spatial model compared to the non-spatial model is not an inherent flaw, but rather a reason to distrust the non-spatial model which suffers from undercoverage. Restricted spatial regression methods only exacerbate the undercoverage, since they preserve the non-spatial posterior mean but decrease the posterior variance (Khan and Calder, 2022).

For the SAR analysis, the efficiency result in (13) is not guaranteed as the analysis spatial structure  $W_\phi^{-1}$  does not match  $V_\phi^{-1}$  in the true data generating model. Nonetheless, the unconditioned spatial model obtains lower mean squared errors and credible interval coverage rates closer to the nominal level compared to the non-spatial model (Table 1). Therefore, a confounded and misspecified

Frequentist Evaluation	$\beta_{01}$	$\beta_{02}$	$\beta_{03}$	$\beta_{11}$	$\beta_{12}$	$\beta_{13}$
MSE( $\mathbb{E}[\beta_{NS}   Y, X_1]$ )	1.513	1.168	1.517	0.076	0.111	0.095
MSE( $\mathbb{E}[\beta_S   Y, X_1]$ ), CAR Prior	1.435	1.065	1.453	0.050	0.090	0.054
MSE( $\mathbb{E}[\beta_S   Y, X_1]$ ), SAR Prior	1.507	1.131	1.523	0.056	0.095	0.062
MSE( $\mathbb{E}[\beta_S   Y, X_1, A, P]$ ), CAR Prior	1.401	1.062	1.458	0.049	0.090	0.050
MSE( $\mathbb{E}[\beta_S   Y, X_1, A, P]$ ), SAR Prior	1.516	1.167	1.687	0.054	0.095	0.056
Coverage( $\beta_{NS}$ )	0.373	0.433	0.423	0.723	0.593	0.667
Coverage( $\beta_S$ ), CAR Prior	0.867	0.923	0.873	0.917	0.763	0.887
Coverage( $\beta_S$ ), SAR Prior	0.983	0.993	0.963	0.867	0.683	0.830
Coverage( $\beta_S   A, P$ ), CAR Prior	0.907	0.950	0.940	0.887	0.713	0.887
Coverage( $\beta_S   A, P$ ), SAR Prior	0.980	0.993	0.973	0.767	0.523	0.690
$\mathbb{E}[\text{Var}(\beta_{NS}   Y, X_1)]$	0.109	0.108	0.108	0.027	0.026	0.027
$\mathbb{E}[\text{Var}(\beta_S   Y, X_1)]$ , CAR Prior	1.006	0.963	0.937	0.039	0.038	0.037
$\mathbb{E}[\text{Var}(\beta_S   Y, X_1)]$ , SAR Prior	2.082	2.100	2.081	0.032	0.032	0.032
$\mathbb{E}[\text{Var}(\beta_S   Y, X_1, A, P)]$ , CAR Prior	1.054	1.054	1.353	0.034	0.034	0.034
$\mathbb{E}[\text{Var}(\beta_S   Y, X_1, A, P)]$ , SAR Prior	1.983	1.983	2.569	0.020	0.020	0.017

TABLE 1. Frequentist evaluation of point estimates and 95% credible intervals from non-spatial and spatial CAR models across 300 datasets generated under a CAR spatial data generation model on a map of Californian counties.

spatial effect may still be preferable to none for estimation, albeit at the cost of large posterior variance inflation for the intercept terms. In practice, we recommend fitting multiple spatial models and using an information criteria such as DIC (Spiegelhalter et al., 2002) or WAIC (Watanabe, 2010) to perform model selection.

We assess model fit by computing the Kullback-Leiber divergence  $D_{KL}(p(Y_0)||q(Y_0))$  for each dataset and analysis model. Here,  $Y_0$  is an observation from a new realization of the underlying stochastic process conditional on  $X_1$ ,  $p(Y_0)$  is the data generation density, and  $q(Y_0)$  is the predictive density under a analysis model. Marginalizing out  $Z$  in the data generation model from (2) yields  $p(Y_0) = N_{nk}(\text{vec}(Y_0) | X(\beta + \delta), A^T(I_k - P)A \otimes I_n + A^T P A \otimes V_\phi)$ . In the non-spatial model,  $q(Y_0) = N_{nk}(\text{vec}(Y_0) | \text{vec}(X\beta_{NS}), \Sigma_{NS} \otimes I_n)$ . For the conditioned spatial model,  $q(Y_0) = N_{nk}(\text{vec}(Y_0) | \text{vec}(X\beta_S), A^T(I_k - P)A \otimes I_n + A^T P A \otimes W_\phi)$ , and for the unconditioned spatial model,  $q(Y_0 | X_1) = N_{nk}(\text{vec}(Y_0) | \text{vec}(X\beta_S), M^T(I_k - R)M \otimes I_n + M^T R M \otimes W_\phi)$ . We use the aforementioned posterior samples for the non-spatial and unconditioned spatial model along with 20,000 exact samples of  $\beta_S$  in the conditioned spatial model to obtain samples from the posterior distribution of  $D_{KL}(p(Y_0)||q(Y_0))$  for each dataset and analysis model. The density plot of the posterior means in Figure 1 demonstrates that the unconditioned spatial models generally provide a better fit than the non-spatial model. Therefore, the increased posterior variance in the spatial models is a more

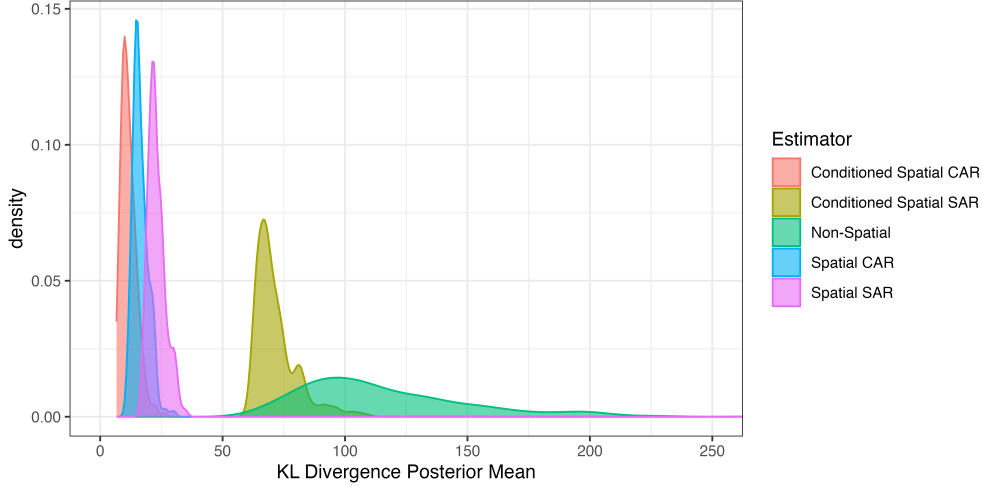


FIGURE 1. Density plot of posterior expectations of  $D_{KL}(p(Y_0)||q(Y_0))$  for the non-spatial model, conditioned CAR and SAR spatial models, and unconditioned CAR and SAR spatial models over 300 datasets simulated from a CAR data generation model.

accurate representation of the true variability in the data generation model. The unconditioned SAR model outperforms the conditioned SAR model, adapting to the misspecified spatial structure.

## 5. OBESITY, DIABETES, AND DIABETES-RELATED CANCER MORTALITY IN US COUNTIES

**5.1. Data Sources and Variables.** We conduct a spatial and non-spatial analysis of US county-level associations between structural characteristics and three health outcomes: obesity prevalence, diabetes prevalence, and diabetes-related cancer mortality. Obesity and diabetes are both associated with increased risk of cancer, treatment complications, and higher mortality rate (Harborg et al., 2024). On the other hand, many epidemiological investigations often study relations between socioeconomic or environmental factors and a single health outcome such as obesity prevalence (see, e.g., Bennett et al., 2011; Salerno et al., 2024; Slack et al., 2014, and references therein), diabetes prevalence (e.g., Cunningham et al., 2018; Hill-Briggs et al., 2020), or cancer mortality rates (e.g., Dong et al., 2022; O’Connor et al., 2018). Furthermore, previous epidemiological studies have demonstrated the need to account for spatial autocorrelation on the county geographic level (e.g., Hipp and Chalise, 2015; Oh et al., 2024; Slack et al., 2014). We seek to consolidate the aforementioned analysis goals while accounting for spatial autocorrelation and more efficiently estimating associations according to the theoretical results of Section 3.2. Our secondary analysis goal is to assess differences in estimation and statistical inference between employing a non-spatial versus spatial analysis model. Estimates of diabetes and obesity age-adjusted prevalence rates among adults aged 20 years or more for 3,142 US counties in 2015 were extracted from the US Diabetes Surveillance System, a database maintained by the Centers for Disease Control and

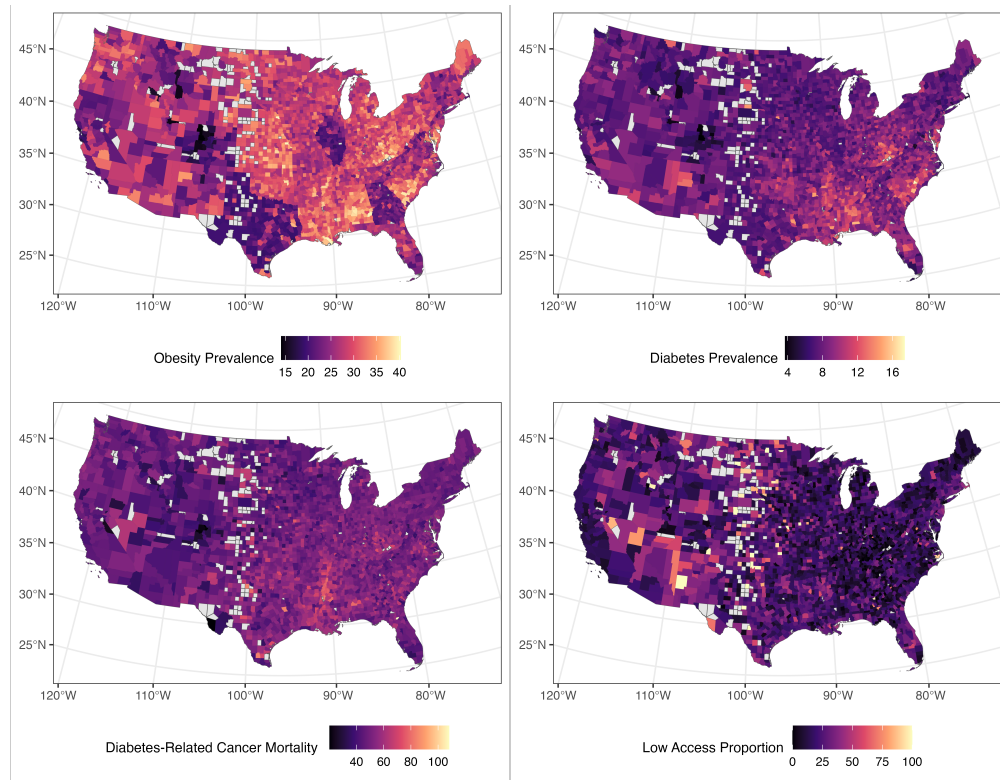


FIGURE 2. US county-level obesity prevalence, diabetes prevalence, diabetes-related cancer mortality rates, and percent of people living in a food desert.

[Prevention \(2015\)](#) (CDC). We define diabetes-related cancer mortality with an underlying cause of death related to liver, pancreatic, endometrial, colorectal, breast, or bladder cancer ([Giovannucci et al., 2010](#)). We obtained age-adjusted mortality rates aggregated from 2010 to 2020 for 3,008 counties based on US resident death certificates classified with the corresponding ICD-10-CM (International Classification of Diseases, Tenth Revision, Clinical Modification) code from the 1999-2020 Underlying Cause of Death WONDER database, made publicly available by the [Centers for Disease Control and Prevention, National Center for Health Statistics \(2021\)](#).

Our analysis accounts for county-level characteristics across five established critical determinants of population health, which include the economic context, healthcare context, natural and built environment, educational context, and population structure ([Myers et al., 2015, 2016](#); [Slack et al., 2014](#)). We account for the economic context of counties through the median household income, poverty rate, and unemployment rate in 2015. The healthcare context is represented by the percentage of the population under 65 years of age without health insurance, the number of primary care physicians per 100,000 people, and the number of outpatient visits per 100,000 people in 2015. Economic and healthcare variables were extracted from the US Department of Health and Human Services 2019-2020 County Level Area Health Resources Files (AHRF), which includes historical data from previous years.

The natural and built environment encapsulates both the food environment and the physical environment, otherwise known as the recreational context. We quantify the food environment by the percentage of the population living in a food desert and the percentage of the population receiving food stamp or Supplemental Nutrition Assistance Program (SNAP) benefits, both estimated for 2015. A person is defined as living in a food desert or low-access area if they live more than one mile from a supermarket or large grocery store in an urban area or more than ten miles in a rural area. Estimates of low access rates were extracted from the Food Environment Atlas, made publicly available by [Economic Research Service \(ERS\), U.S. Department of Agriculture \(USDA\) \(2020\)](#) of the US Department of Agriculture (USDA). The percentages of food stamp or SNAP recipients were drawn from the 2019-2020 AHRF. The recreational context was captured by the age-adjusted percentage of adults aged 18 years or older in the US who are physically inactive in 2015, and the number of recreation and fitness facilities per 1,000 people in 2016. A person is defined as physically inactive if they obtain less than 10 minutes per week of moderate or vigorous activity in each category of physical activity of work, leisure time, and transportation. Data on physical inactivity were drawn from the CDC’s US Diabetes Surveillance System, while data on recreation and fitness facilities was taken from the USDA’s Food Environment Atlas.

The population structure was captured by six variables: the percentage of the population that was non-Hispanic black, the percentage of the population that was Hispanic, the percentage of the population at least 65 years old, the percentage of the population at most 18 years old, the percentage of the population living in urban areas, and the percentage of adults at least 25 years old that hold a high school diploma. Population structure data was extracted from the 2019-2020 AHRF, where all covariates except education were originally sourced from the 2010 Census of the US Census Bureau. The percentage of adults at least 25 years old that hold a high school diploma was sourced from the US Census Bureau’s 2011-2015 American Community Survey’s five-year estimates.

**5.2. Statistical Analysis.** After aggregating all variables into one dataset, we drop counties with missing covariate data and subset to a contiguous region consisting of  $n = 2,960$  US counties for simplicity of analysis. For subsequent analysis, we center and scale the data such that each outcome and covariate has sample mean and standard deviation equal to zero and one, respectively. The three health outcomes as well as food desert exposure are mapped on the final study region in Figure 2, indicating the presence of considerable spatial clustering, such as the high obesity prevalence counties in the East North Central and East South Central states. We first conduct a non-spatial analysis using the non-spatial model in (4). Following the prior recommendations of [Jin et al. \(2007\)](#), we set  $\nu = 3$  and  $\Sigma_0$  as a diagonal matrix where the  $j$ th diagonal element is  $\|(I_n - H)Y_j\|^2 / (n - p - 1)$ . We obtain 10,000 exact posterior samples of  $\beta_{NS}$  and  $\Sigma_{NS}$  by simulating  $\Sigma_{NS} \sim \text{IW}(\nu_\star, \Sigma_\star)$  and then drawing one instance of  $\beta_{NS} \sim N_{pk} \left( \text{vec} \left( \widehat{\beta}_{NS} \right), \Sigma_{NS} \otimes (X^T X)^{-1} \right)$  for each sampled value of  $\Sigma_{NS}$ .

Turning to spatial analysis, we first assess spatial autocorrelation by computing Moran’s  $I$  and Geary’s  $C$  using the residuals of an ordinary least squares linear model for each outcome (Banerjee et al., 2015). Each statistic is significant under 10,000 random permutations (p-value = 1/10,001), indicating that the estimates from the non-spatial analysis model do not account for significant spatial dependence in all three health outcomes. To implement (6), we set the joint prior as in (7) with  $\nu = 3$ ,  $\lambda_R = 0.001$ , and  $\Sigma_0$  identical to the non-spatial model. We place a spatial CAR prior on the random effects by setting  $W_\phi^{-1} = c(D_W - \alpha W)$  with the neighbor and adjacency matrices of the study region,  $\alpha = 0.99$ , and  $c = 0.3963$ . Although there are numerous choices for the spatial prior, we obtained a better fit quantified by a lower DIC using this CAR prior than a SAR spatial prior as in the simulation experiment with  $W_\phi^{-1} = c(I_n - \alpha \tilde{W})(I_n - \alpha \tilde{W})^T$ ,  $\alpha = 0.99$  and  $c = 41.41$ .

We employ the Metropolis within Gibbs sampling scheme detailed in Appendix D with proposal hyperparameters  $s_1 = 0.05$ ,  $s_2 = 0.05$ , and  $s_3 = 0.45$  to obtain  $10,000 \times 4$  chains = 40,000 posterior samples of  $\{\beta_S, \gamma, M, R\}$ . One sample is saved every five update loops to reduce sampling autocorrelation and conserve computer memory. MCMC convergence is assessed via the  $\hat{R}$  and effective sample size statistics computed using the `rstan` package in R. The  $\hat{R}$  statistic is below the recommended threshold of 1.01 and the effective sample size exceeds 1000 for all sampled parameters (Vehtari et al., 2021). Coefficients are deemed statistically significant if the corresponding 95% highest posterior density credible interval does not contain zero.

**5.3. Results.** Table 2 lists the standardized coefficient estimates for the spatial analysis model, indicating that diabetes prevalence in US counties has a moderate positive association with higher percentages of adults that are physically inactive ( $\hat{\beta}_S = 0.47$ ; 95% CI: 0.44, 0.50) and a weak association with percent of non-Hispanic black residents ( $\hat{\beta}_S = 0.22$ ; 95% CI: 0.17, 0.27). Other statistically significant predictors of diabetes prevalence include median income, unemployment rate, outpatient visit rate, percentage SNAP recipients, density of recreation facilities, percentage of residents at least 65 years of age, percentage of residents at most 18 years of age, and percentage of residents in urban areas. Outpatient visit rate and percent of residents 18 years old or younger are significant in the spatial model but not in the non-spatial model, whereas percentage of Hispanic residents is significant in the non-spatial model but not in the non-spatial model (Table 3).

Higher county obesity prevalence rates correlates with higher rates of physical inactivity ( $\hat{\beta}_S = 0.47$ ; 95% CI: 0.44, 0.50), higher proportion of non-Hispanic black residents ( $\hat{\beta}_S = 0.11$ ; 95% CI: 0.07, 0.16), lower median income ( $\hat{\beta}_S = -0.15$ ; 95% CI: -0.21, -0.097), and uninsured rate ( $\hat{\beta}_S = -0.18$ ; 95% CI: -0.23, -0.13). Other significant independent variables weakly associated with higher obesity prevalence include density of primary care physicians, percentage of Hispanic residents, percentage of residents at least 65 years of age, percentage of residents at most 18 years of age, and percentage of residents in urban areas. Primary care physician density, percent of residents at least 65 years old, and percent of residents in urban areas are significant in the spatial

Variable	Diabetes	Obesity	Cancer Mortality
Intercept	1.8e-03 (-0.12, 0.12)	2.2e-05 (-0.11, 0.1)	-8e-03 (-0.17, 0.14)
Poverty Rate	0.031 (-0.039, 0.098)	-0.058 (-0.12, 2.5e-03)	-0.043 (-0.13, 0.042)
Median Income	-0.093 (-0.16, -0.032)	-0.15 (-0.21, -0.097)	-0.18 (-0.26, -0.099)
Unemployment	0.061 (0.017, 0.11)	9.4e-03 (-3e-02, 0.047)	-0.053 (-0.11, 3.5e-03)
Uninsured Rate	-0.011 (-0.067, 0.045)	-0.18 (-0.23, -0.13)	-0.1 (-0.17, -3e-02)
PCP Density	-0.022 (-0.054, 0.011)	-0.045 (-0.074, -0.017)	-3e-02 (-0.071, 0.011)
Outpatient Visits	3e-02 (1.4e-03, 0.057)	0.024 (-1.4e-04, 0.048)	5.4e-03 (-0.029, 0.041)
Low Access	0.024 (-1.2e-03, 0.052)	0.018 (-4.6e-03, 0.042)	0.024 (-9.1e-03, 0.057)
SNAP Assistance	0.089 (0.028, 0.15)	0.029 (-0.027, 0.083)	0.32 (0.25, 0.4)
Physical Inactivity	0.47 (0.44, 0.5)	0.47 (0.44, 0.5)	0.046 (8.3e-03, 0.085)
Recreation Facilities	-4e-02 (-0.068, -0.012)	-0.011 (-0.035, 0.014)	-0.015 (-5e-02, 2e-02)
Percent NH-Black	0.22 (0.17, 0.27)	0.11 (7e-02, 0.16)	0.15 (0.084, 0.21)
Percent Hispanic	-0.052 (-0.11, 5.8e-03)	-0.081 (-0.13, -3e-02)	-0.15 (-0.22, -0.074)
Percent $\geq$ 65 years	-0.091 (-0.13, -0.049)	-0.064 (-0.1, -0.027)	0.073 (0.021, 0.13)
Percent $\leq$ 18 years	0.084 (0.044, 0.13)	0.094 (0.058, 0.13)	0.088 (0.035, 0.14)
Urban Percent	0.085 (0.046, 0.12)	0.069 (0.036, 0.1)	0.061 (0.012, 0.11)
HS Diploma Rate	0.047 (-9.8e-03, 0.1)	-0.017 (-0.066, 0.033)	-0.12 (-0.19, -0.052)

TABLE 2. Spatial model posterior means and 95% highest posterior density credible intervals for regression of US counties’ diabetes prevalence, obesity prevalence, and diabetes-related cancer mortality rates in 2015.

model but not in the non-spatial model, while outpatient visit rate and percent of residents living in food deserts are significant in the non-spatial model but not in the spatial model.

For diabetes-related cancer, the set of significant predictors of county-level mortality was identical between the spatial and non-spatial analysis models. Higher mortality rates are weakly associated with percentage of SNAP recipients ( $\hat{\beta}_S = 0.32$ ; 95% CI: 0.25, 0.40), median income ( $\hat{\beta}_S = -0.18$ ; 95% CI: -0.26, -0.099), rates of high school diploma attainment ( $\hat{\beta}_S = -0.12$ ; 95% CI: -0.19, -0.052), percentage of non-Hispanic black residents ( $\hat{\beta}_S = 0.15$ ; 95% CI: 0.084, 0.21), and percentage of Hispanic residents ( $\hat{\beta}_S = -0.15$ ; 95% CI: -0.22, -0.074). Other significant predictors weakly associated with diabetes-related cancer mortality include percent without health insurance, percentage of adults that are physically inactive, percentage of residents at least 65 years of age, percentage of residents at most 18 years of age, and percentage of residents in urban areas.

## 6. DISCUSSION

This manuscript formally investigates spatial confounding in the presence of multivariate dependencies among outcomes. Our core takeaway is that a spatial model afflicted by spatial confounding

Variable	Diabetes	Obesity	Cancer Mortality
Intercept	5.9e-06 (-0.022, 0.024)	-1.9e-04 (-0.024, 0.025)	-3.9e-05 (-3e-02, 3e-02)
Poverty Rate	-0.043 (-0.1, 0.017)	-6e-02 (-0.12, 7.8e-03)	-0.042 (-0.12, 0.037)
Median Income	-0.049 (-0.099, 3.3e-04)	-0.19 (-0.24, -0.13)	-9e-02 (-0.16, -0.026)
Unemployment	0.1 (0.068, 0.14)	-0.014 (-0.049, 0.024)	-0.11 (-0.15, -0.064)
Uninsured Rate	0.027 (-7.7e-03, 6e-02)	-0.29 (-0.32, -0.25)	-0.058 (-0.1, -0.014)
PCP Density	-0.016 (-0.046, 0.015)	-0.016 (-0.047, 0.017)	-0.069 (-0.11, -0.028)
Outpatient Visits	0.023 (-3.2e-03, 0.049)	0.032 (4.2e-03, 6e-02)	0.042 (9.7e-03, 0.079)
Low Access	0.015 (-0.011, 0.038)	0.046 (0.021, 0.073)	0.047 (0.015, 8e-02)
SNAP Assistance	0.17 (0.12, 0.22)	2e-03 (-0.054, 0.053)	0.31 (0.25, 0.38)
Physical Inactivity	0.51 (0.48, 0.53)	0.6 (0.58, 0.63)	0.089 (0.054, 0.12)
Recreation Facilities	-0.057 (-0.084, -0.029)	-2e-02 (-0.049, 8.4e-03)	-0.028 (-0.064, 7.5e-03)
Percent NH-Black	0.19 (0.16, 0.22)	0.061 (0.027, 0.092)	0.14 (0.1, 0.19)
Percent Hispanic	-0.084 (-0.12, -0.051)	-0.1 (-0.14, -0.068)	-0.16 (-0.2, -0.11)
Percent $\geq$ 65 years	-0.11 (-0.15, -0.074)	5.5e-03 (-0.032, 0.044)	0.099 (0.052, 0.15)
Percent $\leq$ 18 years	8.5e-03 (-0.023, 0.043)	0.16 (0.12, 0.19)	0.072 (0.032, 0.12)
Urban Percent	0.11 (0.073, 0.14)	0.035 (-2.1e-03, 0.071)	0.092 (0.047, 0.14)
HS Diploma Rate	8.1e-03 (-0.034, 0.053)	0.028 (-2e-02, 0.072)	-0.21 (-0.27, -0.15)

TABLE 3. Non-spatial model regression coefficient posterior means and 95% highest posterior density credible regions.

may still produce more efficient estimates with accurate uncertainty quantification compared to a non-spatial model. Adding a spatial effect may alter significant associations, but is not sufficient reason to discard the spatial model. Our simulation results also reveal that the spatial analysis model is robust to misspecified spatial structures.

To our knowledge, we are the first to use a multivariate spatial model to estimate county-level associations for health outcomes of diabetes, obesity, and cancer in the US simultaneously. Although the set of significant predictors differs between spatial and non-spatial models, the resulting credible intervals do not indicate systematic variance inflation from spatial confounding. Previous non-spatial analysis ([Hipp and Chalise, 2015](#); [Knight et al., 2020](#)) indicates that Hispanics are at higher risk of diabetes, but counties with a higher proportion of Hispanic residents are associated with lower rates of diabetes prevalence. Our analysis indicates that the county-level association may be an artifact of spatial clustering of counties with large Hispanic populations. However, large percentages of Hispanic populations are associated with a decrease in obesity prevalence and diabetes-related cancer mortality rates after accounting for spatial dependence. More research is needed to understand the disparity in the levels of Hispanic association at the individual and county levels.

Although exposure to food deserts was not a significant predictor of any of the three health outcomes after accounting for other county-level characteristics in the spatial model, the county-level percentage of SNAP recipients was a significant predictor of diabetes-related cancer mortality with the largest magnitude standardized coefficient estimate in the spatial model. This result is consistent with those of [Chen and Blackford \(2023\)](#) and [Hong et al. \(2024\)](#), which warrant further investigation into the potential causal role that food insecurity plays in related cancer treatment outcomes at the individual and county level. [Oh et al. \(2024\)](#) reports lack of a global association between food environment measures and county-level diabetes or obesity rates, but demonstrates that methods such as geographically weighted regression can identify specific counties that may benefit from regional initiatives such as reducing unhealthy food outlets, introducing more supermarkets or improving park access.

## 7. SUPPLEMENTAL MATERIAL

All computer programs required to reproduce the simulation and data analysis in this manuscript are available at <https://github.com/Ky-Wu/spatial-confounding>.

## REFERENCES

- D. R. M. Azevedo, M. O. Prates, and D. Bandyopadhyay. MSPOCK: Alleviating Spatial Confounding in Multivariate Disease Mapping Models. *Journal of Agricultural, Biological and Environmental Statistics*, 26(3):464–491, Sept. 2021. ISSN 1085-7117, 1537-2693. doi: 10.1007/s13253-021-00451-5.
- S. Banerjee. Modeling massive spatial datasets using a conjugate Bayesian linear modeling framework. *Spatial Statistics*, 37:100417, June 2020. ISSN 2211-6753. doi: 10.1016/j.spasta.2020.100417.
- S. Banerjee, B. P. Carlin, and A. E. Gelfand. *Hierarchical Modeling and Analysis for Spatial Data*. Number 135 in Monographs on Statistics and Applied Probability. CRC Press, Taylor & Francis Group, Boca Raton, second edition edition, 2015. ISBN 978-1-4398-1917-3.
- K. J. Bennett, J. C. Probst, and C. Pumkam. Obesity among working age adults: The role of county-level persistent poverty in rural disparities. *Health & Place*, 17(5):1174–1181, Sept. 2011. ISSN 13538292. doi: 10.1016/j.healthplace.2011.05.012.
- Centers for Disease Control and Prevention. U.S. Diabetes Surveillance System, 2015.
- Centers for Disease Control and Prevention, National Center for Health Statistics. Mortality 1999-2020 on CDC WONDER Online Database, 2021.
- K. Y. Chen and A. L. Blackford. County-level food insecurity to predict cancer incidence and mortality in the United States, 2015-2020. *Journal of Clinical Oncology*, June 2023. doi: 10.1200/JCO.2023.41.16\_suppl.10539.
- S. A. Cunningham, S. A. Patel, G. L. Beckles, L. S. Geiss, N. Mehta, H. Xie, and G. Imperatore. County-level Contextual Factors Associated with Diabetes Incidence in the United States. *Annals*

- of epidemiology*, 28(1):20–25.e2, Jan. 2018. ISSN 1047-2797. doi: 10.1016/j.annepidem.2017.11.002.
- A. Datta, S. Banerjee, J. S. Hodges, and L. Gao. Spatial Disease Mapping Using Directed Acyclic Graph Auto-Regressive (DAGAR) Models. *Bayesian Analysis*, 14(4):1221–1244, Dec. 2019. ISSN 1936-0975, 1931-6690. doi: 10.1214/19-BA1177.
- W. Dong, W. P. Bensken, U. Kim, J. Rose, Q. Fan, N. K. Schiltz, N. A. Berger, and S. M. Koroukian. Variation in and Factors Associated With US County-Level Cancer Mortality, 2008-2019. *JAMA Network Open*, 5(9):e2230925, Sept. 2022. ISSN 2574-3805. doi: 10.1001/jamanetworkopen.2022.30925.
- E. Dupont, S. N. Wood, and N. H. Augustin. Spatial+: A novel approach to spatial confounding. *Biometrics*, 78(4):1279–1290, 2022. ISSN 1541-0420. doi: 10.1111/biom.13656.
- Economic Research Service (ERS), U.S. Department of Agriculture (USDA). Food Environment Atlas, 2020.
- L. Gao, A. Datta, and S. Banerjee. Hierarchical multivariate directed acyclic graph autoregressive models for spatial disease mapping. *Statistics in Medicine*, 41(16):3057–3075, 2022.
- B. Gilbert, E. L. Ogburn, and A. Datta. Consistency of common spatial estimators under spatial confounding. *Biometrika*, 112(2):asae070, Mar. 2025. ISSN 1464-3510. doi: 10.1093/biomet/asae070.
- E. Giovannucci, D. M. Harlan, M. C. Archer, R. M. Bergenstal, S. M. Gapstur, L. A. Habel, M. Pollak, J. G. Regensteiner, and D. Yee. Diabetes and Cancer. *Diabetes Care*, 33(7):1674–1685, July 2010. ISSN 0149-5992. doi: 10.2337/dc10-0666.
- Y. Guan, G. L. Page, B. J. Reich, M. Ventrucci, and S. Yang. Spectral adjustment for spatial confounding. *Biometrika*, 110(3):699–719, Sept. 2023. ISSN 1464-3510. doi: 10.1093/biomet/asac069.
- S. Harborg, K. A. Kjærgaard, R. W. Thomsen, S. Borgquist, D. Cronin-Fenton, and C. F. Hjorth. New Horizons: Epidemiology of Obesity, Diabetes Mellitus, and Cancer Prognosis. *The Journal of Clinical Endocrinology & Metabolism*, 109(4):924–935, Apr. 2024. ISSN 0021-972X. doi: 10.1210/clinem/dgad450.
- F. Hill-Briggs, N. E. Adler, S. A. Berkowitz, M. H. Chin, T. L. Gary-Webb, A. Navas-Acien, P. L. Thornton, and D. Haire-Joshu. Social Determinants of Health and Diabetes: A Scientific Review. *Diabetes Care*, 44(1):258–279, Nov. 2020. ISSN 0149-5992. doi: 10.2337/dci20-0053.
- J. A. Hipp and N. Chalise. Spatial Analysis and Correlates of County-Level Diabetes Prevalence, 2009–2010. *Preventing Chronic Disease*, 12:140404, Jan. 2015. ISSN 1545-1151. doi: 10.5888/pcd12.140404.
- J. S. Hodges and B. J. Reich. Adding Spatially-Correlated Errors Can Mess Up the Fixed Effect You Love. *The American Statistician*, 64(4):325–334, Nov. 2010. ISSN 0003-1305. doi: 10.1198/tast.2010.10052.

- Y.-R. Hong, R. Wang, S. Case, A. Jo, K. Turner, and K. M. Ross. Association of food insecurity with overall and disease-specific mortality among cancer survivors in the US. *Supportive Care in Cancer*, 32(5):1–8, Apr. 2024. ISSN 1433-7339. doi: 10.1007/s00520-024-08495-2.
- J. Hughes and M. Haran. Dimension Reduction and Alleviation of Confounding for Spatial Generalized Linear Mixed Models. *Journal of the Royal Statistical Society Series B: Statistical Methodology*, 75(1):139–159, Jan. 2013. ISSN 1369-7412. doi: 10.1111/j.1467-9868.2012.01041.x.
- F. K. C. Hui and H. D. Bondell. Spatial Confounding in Generalized Estimating Equations. *The American Statistician*, 76(3):238–247, July 2022. ISSN 0003-1305. doi: 10.1080/00031305.2021.2009372.
- X. Jin, S. Banerjee, and B. P. Carlin. Order-Free Co-Regionalized Areal Data Models with Application to Multiple-Disease Mapping. *Journal of the Royal Statistical Society Series B: Statistical Methodology*, 69(5):817–838, Nov. 2007. ISSN 1369-7412. doi: 10.1111/j.1467-9868.2007.00612.x.
- K. Khan and C. Berrett. Re-thinking Spatial Confounding in Spatial Linear Mixed Models, 2023.
- K. Khan and C. A. Calder. Restricted Spatial Regression Methods: Implications for Inference. *Journal of the American Statistical Association*, 117(537):482–494, Jan. 2022. ISSN 0162-1459. doi: 10.1080/01621459.2020.1788949.
- G. M. Knight, G. Spencer-Bonilla, D. M. Maahs, M. R. Blum, A. Valencia, B. Z. Zuma, P. Prahalad, A. Sarraju, F. Rodriguez, and D. Scheinker. Multimethod, multidataset analysis reveals paradoxical relationships between sociodemographic factors, Hispanic ethnicity and diabetes. *BMJ Open Diabetes Research & Care*, 8(2):e001725, Nov. 2020. ISSN 2052-4897. doi: 10.1136/bmjdr-2020-001725.
- Y. C. MacNab. Linear models of coregionalization for multivariate lattice data: a general framework for coregionalized multivariate car models. *Statistics in Medicine*, 35(21):3827–3850, 2016. doi: <https://doi.org/10.1002/sim.6955>. URL <https://onlinelibrary.wiley.com/doi/abs/10.1002/sim.6955>.
- Y. C. MacNab. Some recent work on multivariate Gaussian Markov random fields (with discussion). *TEST: An Official Journal of the Spanish Society of Statistics and Operations Research*, 27(3): 497–541, September 2018. doi: 10.1007/s11749-018-0605-3. URL [https://ideas.repec.org/a/spr/testjl/v27y2018i3d10.1007\\_s11749-018-0605-3.html](https://ideas.repec.org/a/spr/testjl/v27y2018i3d10.1007_s11749-018-0605-3.html).
- C. A. Myers, T. Slack, C. K. Martin, S. T. Broyles, and S. B. Heymsfield. Regional disparities in obesity prevalence in the United States: A spatial regime analysis: Regional Disparities in Adult Obesity. *Obesity*, 23(2):481–487, Feb. 2015. ISSN 19307381. doi: 10.1002/oby.20963.
- C. A. Myers, T. Slack, C. K. Martin, S. T. Broyles, and S. B. Heymsfield. Change in Obesity Prevalence across the United States Is Influenced by Recreational and Healthcare Contexts, Food Environments, and Hispanic Populations. *PLOS ONE*, 11(2):e0148394, Feb. 2016. ISSN 1932-6203. doi: 10.1371/journal.pone.0148394.

- J. M. O'Connor, T. Sedghi, M. Dhodapkar, M. J. Kane, and C. P. Gross. Factors Associated With Cancer Disparities Among Low-, Medium-, and High-Income US Counties. *JAMA Network Open*, 1(6):e183146, Oct. 2018. ISSN 2574-3805. doi: 10.1001/jamanetworkopen.2018.3146.
- J. I. Oh, K. J. Lee, and A. Hipp. Food deserts exposure, density of fast-food restaurants, and park access: Exploring the association of food and recreation environments with obesity and diabetes using global and local regression models. *PLOS ONE*, 19(4):e0301121, Apr. 2024. ISSN 1932-6203. doi: 10.1371/journal.pone.0301121.
- C. J. Paciorek. The Importance of Scale for Spatial-Confounding Bias and Precision of Spatial Regression Estimators. *Statistical Science*, 25(1), Feb. 2010. ISSN 0883-4237. doi: 10.1214/10-STS326.
- M. O. Prates, R. M. Assunção, and E. C. Rodrigues. Alleviating Spatial Confounding for Areal Data Problems by Displacing the Geographical Centroids. *Bayesian Analysis*, 14(2), June 2019. ISSN 1936-0975. doi: 10.1214/18-BA1123.
- A. Riebler, S. H. Sørbye, D. Simpson, and H. Rue. An intuitive Bayesian spatial model for disease mapping that accounts for scaling. *Statistical Methods in Medical Research*, 25(4):1145–1165, Aug. 2016. ISSN 0962-2802. doi: 10.1177/0962280216660421.
- P. R. V. O. Salerno, A. Qian, W. Dong, S. Deo, K. Nasir, S. Rajagopalan, and S. Al-Kindi. County-level socio-environmental factors and obesity prevalence in the United States. *Diabetes, Obesity and Metabolism*, 26(5):1766–1774, May 2024. ISSN 1462-8902, 1463-1326. doi: 10.1111/dom.15488.
- D. Simpson, H. Rue, A. Riebler, T. G. Martins, and S. H. Sørbye. Penalising Model Component Complexity: A Principled, Practical Approach to Constructing Priors. *Statistical Science*, 32(1): 1–28, Feb. 2017. ISSN 0883-4237, 2168-8745. doi: 10.1214/16-STS576.
- T. Slack, C. A. Myers, C. K. Martin, and S. B. Heymsfield. The geographic concentration of us adult obesity prevalence and associated social, economic, and environmental factors. *Obesity*, 22(3):868–874, Mar. 2014. ISSN 1930-7381, 1930-739X. doi: 10.1002/oby.20502.
- D. J. Spiegelhalter, N. G. Best, B. P. Carlin, and A. Van Der Linde. Bayesian measures of model complexity and fit. *Journal of the Royal Statistical Society: Series B (Statistical Methodology)*, 64(4):583–639, 2002. ISSN 1467-9868. doi: 10.1111/1467-9868.00353.
- H. Thaden and T. Kneib. Structural Equation Models for Dealing With Spatial Confounding. *The American Statistician*, 72(3):239–252, July 2018. ISSN 0003-1305. doi: 10.1080/00031305.2017.1305290.
- A. Urdangarin, T. Goicoa, T. Kneib, and M. D. Ugarte. A simplified spatial+ approach to mitigate spatial confounding in multivariate spatial areal models. *Spatial Statistics*, 59:100804, Mar. 2024. ISSN 2211-6753. doi: 10.1016/j.spasta.2023.100804.
- A. Vehtari, A. Gelman, D. Simpson, B. Carpenter, and P.-C. Bürkner. Rank-Normalization, Folding, and Localization: An Improved  $\hat{R}$  for Assessing Convergence of MCMC (with Discussion). *Bayesian Analysis*, 16(2), June 2021. ISSN 1936-0975. doi: 10.1214/20-BA1221.

S. Watanabe. Asymptotic Equivalence of Bayes Cross Validation and Widely Applicable Information Criterion in Singular Learning Theory. *Journal of Machine Learning Research*, 11(116): 3571–3594, 2010. ISSN 1533-7928.

K. L. Wu and S. Banerjee. Assessing Spatial Disparities: A Bayesian Linear Regression Approach, Mar. 2025. arXiv:2407.19171.

D. L. Zimmerman and J. M. Ver Hoef. On Deconfounding Spatial Confounding in Linear Models. *The American Statistician*, 76(2):159–167, Apr. 2022. ISSN 0003-1305. doi: 10.1080/00031305.2021.1946149.

#### APPENDIX A. CONDITIONAL POSTERIOR DISTRIBUTION OF $\beta_S$ AND $\gamma$ IN SPATIAL ANALYSIS MODEL

Let  $M_0 \in \mathbb{R}^{(p+1)k \times (p+1)k}$  be positive definite,  $m_0 \in \mathbb{R}^{n(p+1) \times 1}$ , and  $W_\phi \in \mathbb{R}^{n \times n}$  be positive definite. If  $\pi(\beta_S, \gamma, M, R) = N_{pk}(\text{vec}(\beta_S) | M_0 m_0, M_0) \times N_{nk}(\text{vec}(\gamma) | 0_{nk}, M^T R M \otimes W_\phi) \times \pi(M, R)$  is the prior for (6), then the joint posterior distribution is equivalent to that of the augmented model (Banerjee, 2020),

$$\underbrace{\begin{bmatrix} \text{vec}(Y) \\ M_0 m_0 \\ 0_{nk} \end{bmatrix}}_{y_\star} = \underbrace{\begin{bmatrix} I_k \otimes X & I_{nk} \\ I_{(p+1)k} & 0_{(p+1)k \times nk} \\ 0_{nk \times (p+1)k} & I_{nk} \end{bmatrix}}_{X_\star} \underbrace{\begin{bmatrix} \text{vec}(\beta_S) \\ \text{vec}(\gamma) \end{bmatrix}}_{\beta_\star} + \underbrace{\begin{bmatrix} \eta \\ \eta_{\beta_S} \\ \eta_\phi \end{bmatrix}}_{\eta_\star}, \quad \eta_\star \sim N_{k(2n+p+1)}(0_{k(2n+p+1)}, V_{y_\star}),$$

where  $V_{y_\star} = \begin{bmatrix} M^T(I_k - R)M \otimes I_n & 0_{nk \times (p+1)k} & 0_{nk \times nk} \\ 0_{(p+1)k \times nk} & M_0 & 0_{(p+1)k \times nk} \\ 0_{nk \times nk} & 0_{nk \times (p+1)k} & M^T R M \otimes W_\phi \end{bmatrix}$  and the prior  $\pi(\beta_\star, M, R) = \pi(M, R)$ .

By standard Bayesian linear regression computations, the conditional posterior  $\pi(\beta_\star | y_\star, M, R, X_1) = N_{(n+p+1)k}(\beta_\star | F_{\beta_\star} f_{\beta_\star}, F_{\beta_\star})$  where  $f_{\beta_\star} = X_\star^T V_{y_\star}^{-1} y_\star$  and  $F_{\beta_\star} = (X_\star V_{y_\star}^{-1} X_\star)^{-1}$ . Calculation yields

$$F_{\beta_\star}^{-1} = \begin{bmatrix} M_0^{-1} + M^{-1}(I_k - R)^{-1}M^{-T} \otimes X^T X & M^{-1}(I_k - R)^{-1}M^{-T} \otimes X^T, \\ M^{-1}(I_k - R)^{-1}M^{-T} \otimes X & M^{-1}(I_k - R)^{-1}M^{-T} \otimes I_n + M^{-1}R^{-1}M^{-T} \otimes W_\phi^{-1} \end{bmatrix},$$

$$f_{\beta_\star} = \begin{bmatrix} (M^{-1}(I_k - R)^{-1}M^{-T} \otimes X^T) \text{vec}(Y) + m_0 \\ (M^{-1}(I_k - R)^{-1}M^{-T} \otimes I_n) \text{vec}(Y). \end{bmatrix}.$$

When  $\pi(\beta_S, \gamma, M, R) \propto N_{nk}(\text{vec}(\gamma) | 0_{nk}, M^T R M \otimes W_\phi) \times \pi(M, R)$ , then

$$f_{\beta_\star} = \begin{bmatrix} \text{vec}(X^T Y M^{-1}(I_k - R)^{-1}M^{-T}) \\ \text{vec}(Y M^{-1}(I_k - R)^{-1}M^{-T}) \end{bmatrix}, \quad F_{\beta_\star} = \begin{bmatrix} M^T(I_k - R)M \otimes (X^T X)^{-1} + B_1 B_2 B_1^T & -B_1 B_2 \\ -B_2 B_1^T & B_2 \end{bmatrix}, \quad (15)$$

where  $B_1 = I_k \otimes (X^T X)^{-1} X^T$  and  $B_2^{-1} = M^{-1}(I_k - R)^{-1}M^{-T} \otimes (I - H) + M^{-1}R^{-1}M^{-T} \otimes W_\phi^{-1}$ . Evaluating  $F_{\beta_\star} f_{\beta_\star} = (X_\star V_{y_\star}^{-1} X_\star)^{-1} X_\star V_{y_\star}^{-1} y_\star$  results in the expressions for  $\mathbb{E}[\beta_S | Y, M, R, X_1]$  and  $\mathbb{E}[\text{vec}(\gamma) | Y, M, R, X_1]$  in (9).

The upper-left block element of  $F_{\beta_\star}$  is the conditional posterior variance  $\text{Var}(\beta_S | Y, M, R, X_1)$ . Since  $W_\phi^{-1}$  is assumed to be positive definite and  $I_n - H$  is positive semi-definite, by spectral decomposition, there exists an orthogonal matrix  $Q$  and diagonal matrix  $D = \text{diag}(d_1, \dots, d_n)$  with  $d_i \geq 0$  for all  $i$  such that  $W_\phi^{1/2}(I - H)W_\phi^{1/2} = QDQ^\top$ . Set  $U = W_\phi^{1/2}Q$ , then  $U$  is invertible,  $W_\phi^{-1} = U^{-\top}U^{-1}$ ,  $I_n - H = U^{-\top}DU^{-1}$ , and the conditional posterior variance of  $\beta_S$  can be expressed as

$$\text{Var}(\text{vec}(\beta_S) | Y, M, R, X_1) = M^\top(I_k - R)M \otimes (X^\top X)^{-1} + S_1 \left( (I_k - R)^{-1} \otimes D + R^{-1} \otimes I_n \right)^{-1} S_1^\top, \quad (16)$$

where  $S_1 = M^\top \otimes (X^\top X)^{-1} X^\top U$ .

## APPENDIX B. LIMITING POSTERIOR DISTRIBUTION OF $M$

Under the spatial analysis model of (6), let the prior be given by (7). We show that the limit of  $\pi(\beta_S, M^\top M | Y, R, X_1)$  as  $r \rightarrow 1^-$  is equal to the result in (12). Set  $\beta_\star = (\text{vec}(\beta_S)^\top, \text{vec}(\gamma)^\top)^\top$ , and let  $f_{\beta_\star}$  and  $F_{\beta_\star}$  be given by (15). By the use of an augmented model as in Appendix A,

$$\begin{aligned} \pi(\beta_\star, M | Y, R, X_1) &\propto \pi(Y | \beta_\star, M, R, X_1) \pi(\beta_\star, M | R, X_1) \\ &\propto \exp \left( -\frac{1}{2} \left( \beta_\star^\top F_{\beta_\star}^{-1} \beta_\star - 2\beta_\star^\top f_{\beta_\star} + y_\star^\top V_{y_\star}^{-1} y_\star \right) \right) |M^\top M|^{-n} \times \pi(M) \\ &\propto N_{(n+p+1)k}(\beta_\star | F_{\beta_\star} f_{\beta_\star}, F_{\beta_\star}) \times \exp \left( -\frac{1}{2} \left( y_\star^\top V_{y_\star}^{-1} y_\star - f_{\beta_\star}^\top F_{\beta_\star} f_{\beta_\star} \right) \right) |M^\top M|^{-\frac{n-p-1}{2}} \times \pi(M). \end{aligned}$$

Hence,  $\pi(M^\top M | Y, R, X_1) \propto \exp \left( -\frac{1}{2} \left( y_\star^\top V_{y_\star}^{-1} y_\star - f_{\beta_\star}^\top F_{\beta_\star} f_{\beta_\star} \right) \right) |M^\top M|^{-\frac{n-p-1}{2}} \times \text{IW}(M^\top M | \nu, \nu \Sigma_0)$ . Matrix calculations reveals that  $y_\star^\top V_{y_\star}^{-1} y_\star - f_{\beta_\star}^\top F_{\beta_\star} f_{\beta_\star} = \text{vec}(YM^{-1})^\top Q_1 \text{vec}(YM^{-1})$ , where

$$Q_1 = (I_k - R)^{-1} \otimes (I_n - H) - \left( (I_k - R)^{-1} \otimes (I_n - H) \right) B^{-1} (I_k \otimes (I_n - H))$$

and  $B = I_k \otimes (I_n - H) + R^{-1} (I_k - R) \otimes W_\phi^{-1}$ . By spectral decomposition, there exists an orthogonal matrix  $Q$  and diagonal matrix  $D = \text{diag}(d_1, \dots, d_n)$  with  $d_i \geq 0$  for all  $i$  such that  $W_\phi^{1/2}(I - H)V_\phi^{1/2} = QDQ^\top$ . Set  $U = W_\phi^{1/2}Q$ , then  $I_n - H = U^{-\top}DU^{-1}$ ,  $W_\phi^{-1} = U^{-\top}U^{-1}$ , and

$$Q_1 = (I_k \otimes U^{-\top}) \left( (I_k - R)^{-1} \otimes D - \left( (I_k - R)^{-1} \otimes D^2 \right) \left( I_k \otimes D + R^{-1} (I_k - R) \otimes I_n \right)^{-1} \right) (I_k \otimes U^{-1})$$

Let  $R_{ii} = r \in (0, 1)$  for all  $i = 1, \dots, k$ . For any given  $d_j$ ,  $\frac{d_j}{1-r} - \frac{d_j^2}{(1-r)(d_j+(1-r)/r)} = \frac{d_j}{rd_{j+1-r}}$ , which converges to 0 as  $r \rightarrow 1^-$  if  $d_j = 0$  and converges to 1 if  $d_j > 0$ . Therefore,  $\lim_{r \rightarrow 1^-} Q_1 = I_k \otimes U^{-\top} D^\star U^{-1}$ , where  $D^\star$  is a  $n \times n$  diagonal matrix with  $D_{ii}^\star = \mathbf{I}(d_i > 0)$  for all  $i = 1, \dots, n$ . Further simplification shows that  $\lim_{r \rightarrow 1^-} (y_\star^\top V_{y_\star}^{-1} y_\star - f_{\beta_\star}^\top F_{\beta_\star} f_{\beta_\star}) = \text{tr}(Y^\top U^{-\top} D^\star U^{-1} Y M^{-1} M^{-\top})$ . The final result is

$$\lim_{r \rightarrow 1^-} \pi(M^\top M | Y, r, X_1) \propto |M^\top M|^{-\frac{\nu+n-p-1}{2}} \exp \left( -\frac{1}{2} \text{tr} \left( (\nu \Sigma_0 + Y^\top U^{-\top} D^\star U^{-1} Y) M^{-1} M^{-\top} \right) \right)$$

which identifies as the density of an inverse-Wishart distribution with parameters given by (12).

### APPENDIX C. VARIANCE OF $\widetilde{\beta}_S$ OVER JOINT DENSITY OF $(X, Y, Z)$

Suppose that under the data-generating model,  $\text{Var}(\text{vec}(Y) | X_1) = A^T P A \otimes V_\phi + A^T (I_k - P) A \otimes I_n$ , where  $V_\phi$  is a fixed  $n \times n$  positive definite matrix capturing the true spatial covariance structure of the latent factors,  $A$  is an invertible  $k \times k$  matrix, and  $P = \text{diag}(\rho_1, \dots, \rho_k)$  with  $\rho_i \in (0, 1)$  for  $i = 1, \dots, k$  (such as in the data-generation model discussed in Section 2). Consider the analysis model in (6) with the working spatial covariance matrix  $W_\phi$  equal to the data generation spatial covariance matrix  $V_\phi$ ,  $\widetilde{\beta}_S = \mathbb{E}[\beta_s | Y, M = A, R = P, X_1]$ , and  $\widehat{\gamma} = \mathbb{E}[\gamma | Y, M = A, R = P, X_1]$ . We show that  $\text{Var}(\widetilde{\beta}_{S,ij} | X_1) \leq \text{Var}(\widehat{\beta}_{NS,ij} | X_1)$  for  $i = 0, \dots, p$  and  $j = 1, \dots, k$ . Under the data-generation model,

$$\text{Cov}(\text{vec}(\widehat{\beta}_{NS}), \text{vec}((X^T X)^{-1} X^T \widehat{\gamma}) | X_1) = (A^T P \otimes (X^T X)^{-1} X^T V_\phi (I_n - H)) B^{-1} (A \otimes X (X^T X)^{-1})$$

since  $X^T (I - H) = 0$ . Since  $V_\phi^{-1}$  is assumed to be positive definite and  $I_n - H$  is positive semi-definite, by spectral decomposition, there exists an orthogonal matrix  $Q$  and diagonal matrix  $D = \text{diag}(d_1, \dots, d_n)$  with  $d_i \geq 0$  for all  $i$  such that  $V_\phi^{1/2} (I - H) V_\phi^{1/2} = Q D Q^T$ . Set  $U = V_\phi^{1/2} Q$ , then  $U$  is invertible,  $U^T V_\phi^{-1} U = I_n$ ,  $U^T (I_n - H) U = D$ ,  $V_\phi (I_n - H) = U D U^{-1}$ ,  $(I_n - H) V_\phi (I_n - H) = U^{-T} D^2 U^{-1}$ ,  $B^{-1} = (I_k \otimes U) (I_k \otimes D + P^{-1} (I_k - P) \otimes I_n)^{-1} (I_k \otimes U^T)$ , which means that  $(P \otimes V_\phi (I - H)) B^{-1} = (P \otimes U D) (I_k \otimes D + P^{-1} (I_k - P) \otimes I_n)^{-1} (I_k \otimes U^T)$ .

As a result,  $\text{Cov}(\text{vec}(\widehat{\beta}_{NS}), \text{vec}((X^T X)^{-1} X^T \widehat{\gamma}) | X_1) = (A^T \otimes (X^T X)^{-1} X^T U) M_1 (A \otimes U^T X (X^T X)^{-1})$ , where  $M_1 = (P \otimes D) (I_k \otimes D + P^{-1} (I_k - P) \otimes I_n)^{-1}$ .  $M_1$  is diagonal with positive diagonal elements, so  $\text{Cov}(\text{vec}(\widehat{\beta}_{NS}), \text{vec}((X^T X)^{-1} X^T \widehat{\gamma}) | X_1)$  is symmetric. We now turn to  $\text{Var}(\text{vec}(\widehat{\gamma}) | X_1)$ . From (9),

$$\text{Var}(\text{vec}(\widehat{\gamma}) | X_1) = (A^T \otimes I_n) B^{-1} (P \otimes (I_n - H) V_\phi (I_n - H) + (I_k - P) \otimes (I_n - H)) B^{-1} (A \otimes I_n)$$

Making the aforementioned substitutions for  $V_\phi$ ,  $I_n - H$ , and  $B^{-1}$  yields

$$\begin{aligned} \text{Var}(\text{vec}(\widehat{\gamma}) | X_1) &= (A^T \otimes U) \left( I_k \otimes D + P^{-1} (I_k - P) \otimes I_n \right)^{-1} (P \otimes D^2 + (I_k - P) \otimes D) \\ &\quad \cdot \left( I_k \otimes D + P^{-1} (I_k - P) \otimes I_n \right)^{-1} (A \otimes U^T) \end{aligned}$$

The inner three terms of the product are diagonal matrices and commute. Thus,

$$\text{Var}(\text{vec}(\widehat{\gamma}) | X_1) = (A^T \otimes U) \left( I_k \otimes D + P^{-1} (I_k - P) \otimes I_n \right)^{-2} (P \otimes D^2 + (I_k - P) \otimes D) (A \otimes U^T),$$

Since  $M_1 = (I_k \otimes D + P^{-1} (I_k - P) \otimes I_n)^{-2} (P \otimes D^2 + (I_k - P) \otimes D)$ , this implies from (9) that

$$\text{Var}(\text{vec}(\widetilde{\beta}_S) | X_1) = \text{Var}(\text{vec}(\widehat{\beta}_{NS}) | X_1) - (A^T \otimes (X^T X)^{-1} X^T U) M_1 (A \otimes U^T X (X^T X)^{-1}). \quad (17)$$

Here,  $M_1$  is a positive definite matrix, which means that  $\text{Var}(\text{vec}(\widehat{\beta}_{NS}) | X_1) - \text{Var}(\text{vec}(\widetilde{\beta}_S) | X_1)$  is a positive definite matrix and implies  $\text{Var}(\widetilde{\beta}_{S,ij} | X_1) < \text{Var}(\widehat{\beta}_{NS,ij} | X_1)$  for  $i = 0, \dots, p$  and

$j = 1, \dots, k$ . If  $\mathbb{E}[Z | X] = X\delta$  as well, then  $\mathbb{E}[\widetilde{\beta}_S] = \mathbb{E}[\widehat{\beta}_{NS}] = \beta + \delta$  and

$$\text{Var}(\widetilde{\beta}_{S,ij}) = \mathbb{E}_{X_1} [\text{Var}(\widetilde{\beta}_{S,ij} | X_1)] < \mathbb{E}_{X_1} [\text{Var}(\widehat{\beta}_{NS,ij} | X_1)] = \text{Var}(\widehat{\beta}_{NS,ij}).$$

By the bias-variance decomposition of mean squared error, the claim of (13) follows. Similar calculations reveal that  $\text{Var}(\text{vec}(\widehat{\beta}_{NS}) | X_1) = A^\top(I_k - P)A \otimes (X^\top X)^{-1} + (A^\top \otimes (X^\top X)^{-1} X^\top U)(P \otimes I_n)(A \otimes U^\top X(X^\top X)^{-1})$ . Since  $(P \otimes I_n) - M_1 = ((I_k - P)^{-1} \otimes D + P^{-1} \otimes I_n)^{-1}$ , then by (16),  $\text{Var}(\text{vec}(\widetilde{\beta}_S) | X_1) = \text{Var}(\beta_S | Y, M = A, R = P, X_1)$ .

#### APPENDIX D. METROPOLIS WITHIN GIBBS SAMPLING ALGORITHM FOR SPATIAL ANALYSIS MODEL

Algorithm 3 details a sampling scheme that applies the Gibbs update steps for  $\{\beta, \gamma\}$  and Metropolis update steps for  $\{M, R\}$  provided in Algorithm 1 for the multivariate BYM2 model in (6) when the prior is given by (7). Algorithm 3 takes as inputs the data  $\{X, Y\}$ , prior parameters  $\{W_\phi^{-1}, \nu, \Sigma_0, \lambda_R\}$ , initial values  $\{\beta^{(0)}, \gamma^{(0)}, M^{(0)}, R^{(0)}\}$ , and proposal parameters  $\{s_1, s_2, s_3\}$ . Here, `chol` returns the lower triangular Cholesky factor of a positive definite matrix, `updateBeta` returns  $\beta_S$  from  $\text{vec}(\beta_S) | Y, X_1, \gamma, A, P \sim N_{pk}(\text{vec}((X^\top X)^{-1} X^\top (Y - \gamma)), M^\top(I_k - R)M \otimes (X^\top X)^{-1})$  and `updateGamma` returns  $\gamma$  from  $\text{vec}(\gamma) | Y, X_1, \beta_S, A, P \sim N_{nk}(F_\gamma f_\gamma, F_\gamma)$  where  $F_\gamma = (M^\top \otimes I_n) \left( (I_k - R)^{-1} \otimes I_n + R^{-1} \otimes W_\phi^{-1} \right)^{-1} (M \otimes I_n)$  and  $f_\gamma = (M^{-1}(I_k - R)^{-1} M^{-\top} \otimes I_n) \text{vec}(Y - X\beta_S)$ .

`MHupdateM` updates the lower triangular matrix  $M$  via a Metropolis random walk by proposing the lower triangular  $k \times k$   $M^\star$ , constructed by sampling diagonal elements  $\log(M_{ii}^\star) \sim N(\log(M_{ii}), s_1^2)$  and off-diagonal elements  $M_{ij}^\star \sim N(M_{ij}, s_2^2)$ . If  $M^\star$  is accepted,  $(M^\star)^{-1}$  is also returned for intermediate calculations. Finally, `MHupdateR` performs a Metropolis update of  $R$  by proposing  $R^\star = \text{diag}(r_1^\star, \dots, r_k^\star)$  where  $\log\left(\frac{r_i^\star}{1-r_i^\star}\right) \sim N\left(\log\left(\frac{r_i^\star}{1-r_i^\star}\right), s_3^2\right)$ . To compute the Metropolis acceptance ratios, `MHupdateM` and `MHupdateR` call the functions in Algorithm 2 to compute posterior densities up to a constant. `logLikGammaPrior` computes  $\log \pi(Y | X_1, \beta_S, \gamma, M, R) + \log \pi(\gamma | M, R) + C_1$ , `logMPrior` evaluates  $\log \pi(M) + C_2$ , and `logRPrior` returns  $\log \pi(R) + C_3$ . Here,  $\pi(Y | X_1, \beta_S, \gamma, M, R) = N_{nk}(\text{vec}(Y) | \text{vec}(X\beta_S + \gamma), M^\top(I - R)M \otimes I_n)$ ,  $\pi(\gamma | M, R) = N_{nk}(\text{vec}(\gamma) | 0_{nk}, M^\top R M \otimes W_\phi)$ ,  $\pi(M) = \text{IW}(MM^\top | \nu, \nu\Sigma_0) \times \prod_{i=1}^k M_{ii}^{k-i+1}$ ,  $\pi(R) = \text{PC}(R | \lambda_R)$ , and  $\{C_1, C_2, C_3\}$  is a set of constants that does not depend on model parameters.

---

**Algorithm 1:** Update steps for  $M$  and  $L$  in Metropolis within Gibbs sampling of MBYM2 Model

---

**function** updateBeta( $\gamma, M, R$ ):

```

for  $j = 1, \dots, k$  do
  for  $i = 0, \dots, p$  do
    | Sample  $Z_{ij} \sim N(0, 1)$ .
  Update  $Z \leftarrow Z \text{diag}(\sqrt{1 - r_i}) M$ .
  Set  $\beta \leftarrow \text{forwardsolve}(L_X, M_1 - X^T \gamma)$ ;  $\beta \leftarrow \text{backsolve}(L_X^T, \beta + Z)$ .
return  $\beta$ .

```

**function** updateGamma( $\beta, M, M^{-1}, R$ ):

```

Set  $\gamma \leftarrow Q^T(Y - X\beta)M^{-1}$ .
for  $j = 1, \dots, k$  do
  for  $i = 1, \dots, N$  do
    | Sample  $Z_{ij} \sim N(0, 1)$ ; set  $w_i \leftarrow \frac{1-r_j}{r_j \lambda_i + 1 - r_j}$ ;  $z_i \leftarrow \sqrt{\frac{r_j(1-r_j)}{r_j + (1-r_j)\lambda_i}}$ .
    | Update  $\gamma_{.j} \leftarrow \gamma_{.j} \otimes w$ ;  $Z_{.j} \leftarrow Z_{.j} \otimes z$ . ( $\gamma_{.j}$  denotes the  $j$ th column of  $\gamma$ )
  Update  $\gamma \leftarrow Q(\gamma + Z)M$ .
return  $\gamma$ .

```

**function** MHupdateM( $\beta, \gamma, M, M^{-1}, L, R$ ):

```

Initialize  $M^* \leftarrow 0_{k \times k}$ ;  $\alpha_{MH} \leftarrow 0$ ; sample  $u \sim \text{Unif}(0, 1)$ .
for  $j = 1, \dots, k$  do
  for  $i = j, \dots, k$  do
    | if  $i = j$  then sample  $\log(M_{ii}^*) \sim N(\log(M_{ii}), s_1^2)$ .;
    | else sample  $M_{ij}^* \sim N(M_{ij}, s_2^2)$ .;
  Set  $(M^*)^{-1} \leftarrow \text{forwardsolve}(M^*, I_k)$ . Update
   $\alpha_{MH} \leftarrow \alpha_{MH} + \log \text{LikGammaPrior}(\beta, \gamma, M^*, (M^*)^{-1}, R) + \log \text{MPrior}(M^*)$ .
  Update  $\alpha_{MH} \leftarrow \alpha_{MH} - \log \text{LikGammaPrior}(\beta, \gamma, M, M^{-1}, R) - \log \text{MPrior}(M)$ .
  if  $\log(u) \leq \alpha_{MH}$  then return  $M^*, (M^*)^{-1}$ .
  else return  $M, M^{-1}$ .

```

**function** MHupdateR( $\beta, \gamma, M, M^{-1}, L, R$ ):

```

Initialize  $\alpha_{MH} \leftarrow 0$ ; sample  $u \sim \text{Unif}(0, 1)$ .
for  $i = 1, \dots, k$  do
  | Sample  $\tau \sim N\left(\log\left(\frac{r_i}{1-r_i}\right), s_3^2\right)$ ;  $r_i^* \leftarrow \frac{\exp(\tau)}{1 + \exp(\tau)}$ .
  | Update  $\alpha_{MH} \leftarrow \alpha_{MH} + \log(r_i(1-r_i)) - \log(r_i^*(1-r_i^*))$ .
  Update  $\alpha_{MH} \leftarrow \alpha_{MH} + \log \text{LikGammaPrior}(\beta, \gamma, M, M^{-1}, R_\star) + \log \text{RPrior}(R_\star)$ .
  Update  $\alpha_{MH} \leftarrow \alpha_{MH} - \log \text{LikGammaPrior}(\beta, \gamma, M, M^{-1}, R) - \log \text{RPrior}(R)$ .
  if  $\log(u) \leq \alpha_{MH}$  then return  $R_\star$ .
  else return  $R$ .

```

---

---

**Algorithm 2:** Log-likelihood and prior densities for Metropolis acceptance ratios

---

```
function logLikGammaPrior( $\beta, \gamma, M, M^{-1}, R$ ):
  Initialize  $d \leftarrow 0$ ;  $\Delta \leftarrow Y - X\beta - \gamma$ ;  $\theta \leftarrow W_\phi^{-1/2} \gamma M^{-1}$ .
  for  $j = 1, \dots, k$  do
    for  $i = 1, \dots, N$  do
      Update  $d \leftarrow d - \frac{1}{2} \left( \frac{\Delta_{ij}^2}{1-r_j} + \frac{\theta_{ij}^2}{r_j} \right)$ .
    Update  $d \leftarrow d - \frac{N}{2} \log(r_j(1-r_j)) - 2N \log(M_{jj})$ .
  return  $d$ .

function logMPrior( $L$ ):
  Initialize  $d \leftarrow 0$ .
  Set  $V \leftarrow \text{forwardsolve}(M, \Sigma_0)$ ; update  $V \leftarrow \text{backsolve}(M^T, V)$ .
  for  $i = 1, \dots, k$  do
    Update  $d \leftarrow d - (v+i) \log(M_{ii}) - \frac{v}{2} V_{ii}$ .
  return  $d$ .

function logRPrior( $R$ ):
  Initialize  $d \leftarrow - \left( \sum_{i=1}^k r_i \right) \cdot \left( N - \sum_{j=1}^N \lambda_j^{-1} \right)$ .
  for  $i = 1, \dots, k$  do
    for  $j = 1, \dots, N$  do
      Update  $d \leftarrow d - \log(1 - r_i + r_i/\lambda_j)$ .
  return  $-\lambda_R \sqrt{d}$ .
```

---

---

**Algorithm 3:** Metropolis within Gibbs Sampling for MBYM2 Model

---

```
Given  $Y, X, L_X = \text{chol}(X^T X), I_n - H, W_\phi^{-1}, \nu, \Sigma_0, \lambda_R, \beta^{(0)}, \gamma^{(0)}, M^{(0)}, R^{(0)}, s_1, s_2, s_3$ :
Initialize  $M_1 \leftarrow X^T Y$ ;  $M^{-1} \leftarrow (M^{(0)})^{-1}$ ;  $L \leftarrow \text{chol}(M^{(0)T} M^{(0)})$ .
Solve spectral decomposition  $W_\phi^{-1} = Q\Lambda Q^T$ ,  $\Lambda = \text{diag}(\lambda_1, \dots, \lambda_n)$ . Set  $W_\phi^{-1/2} \leftarrow Q\Lambda^{1/2}Q^T$ .
for  $t = 1, \dots, T$  do
  Set  $\beta^{(t)} \leftarrow \text{updateBeta}(\gamma^{(t-1)}, M^{(t-1)}, P^{(t-1)})$ .
  Set  $\gamma^{(t)} \leftarrow \text{updateGamma}(\beta^{(t)}, M^{(t-1)}, M^{-1}, R^{(t-1)})$ .
  Set  $M^{(t)}, M^{-1}, L \leftarrow \text{MHupdateM}(\beta^{(t)}, \gamma^{(t)}, M^{(t-1)}, M^{-1}, L, R^{(t-1)})$ 
  Set  $R^{(t)} \leftarrow \text{MHupdateR}(\beta^{(t)}, \gamma^{(t)}, M^{(t)}, M^{-1}, L, R^{(t-1)})$ 
```

---